國家同步輻射研究中心
National Synchrotron Radiation Research Center

High Brightness Beam Technology

李安平

線型加速器小組
同步輻射研究中心
2023.07.03

Outline

- High brightness electron beam source
- Electron Source
- Electron guns
- Bunch compressor
- Beam diagnostics

- **High brightness electron beam source**
- Electron Source
- Electron guns
- Bunch compressor
- Beam diagnostics

High Brightness Beam Source

- The brightness of a charged particle beam, defined as the number of electrons within the 4-D phase space volume, dictates its luminosity.
- The wavelength λ of the free-electron laser (FEL) is governed by the emittance ε_n of the electron beam which sets the lower limit on the wavelength deliverable by an FEL.
- As the wavelength of the FEL gets shorter, the required emittance gets lower and thereby brightness increases.
- In the free electron laser , the beam quality is set ultimately by the injector and electron source.

Brightness

$$B = \frac{I}{\varepsilon_{nx}\varepsilon_{ny}}$$

$$\frac{\varepsilon_n}{\gamma} < \frac{\lambda_{FEL}}{4\pi}$$

Any linac based, high brightnees light source contains the following main components:

- electron source →space charge force
- accelerating sections → wake field
- bunch compressor → coherent synchrotron radiation
- undulator to produce FEL radiation
- beam dump

⇨ Increase ε_n !

→ The Injector has to produce lowest possible emittance

Typical Photo-injector

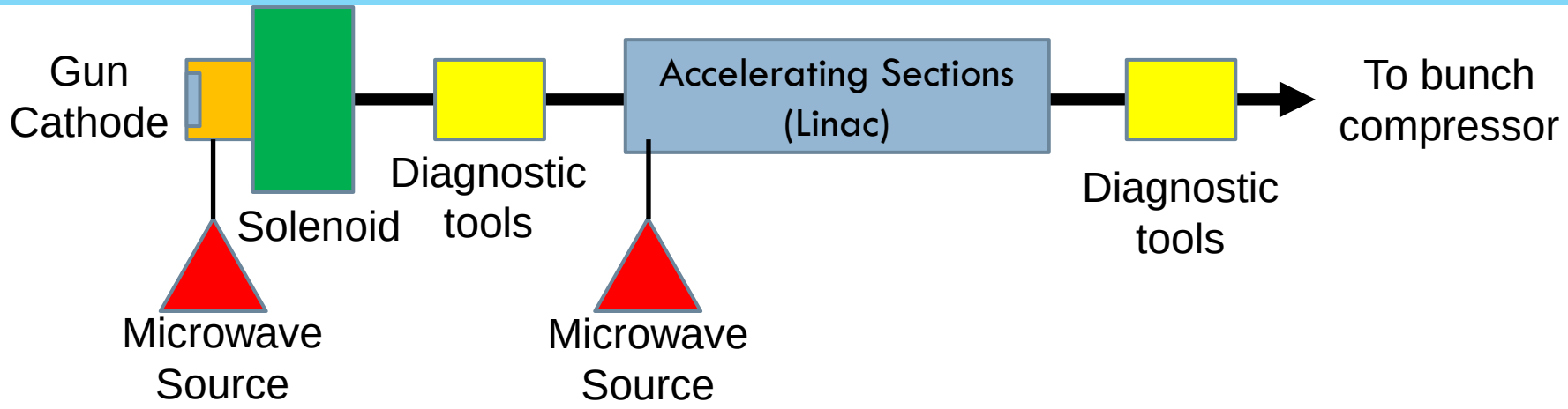

A photo-injector has the following major components:

- **ELECTRON GUN** (either DC or RF) : electron bunches are generated from the cathode and accelerated by DC Electric field or RF field from rest.
- **SOLENOID** : it is used to performs the emittance compensation.
- **DRIVE LASER** : laser pulses are illuminated on the cathode than electrons are emitted from the photocathode .
- **LINEAR ACCELERATOR :** it is used to accelerate the electrons exiting the gun to sufficiently high energy.
- **HV or RF SOURCE :** the power source (such as a klystron) provides EM power for the electron gun and the linac.
- **DIAGNOSTIC TOOLS :** used to characterizes electron beams such as beam profile monitor, current transformer, deflecting cavity, spectrometer magnet,….

NSRRC Photo-injector

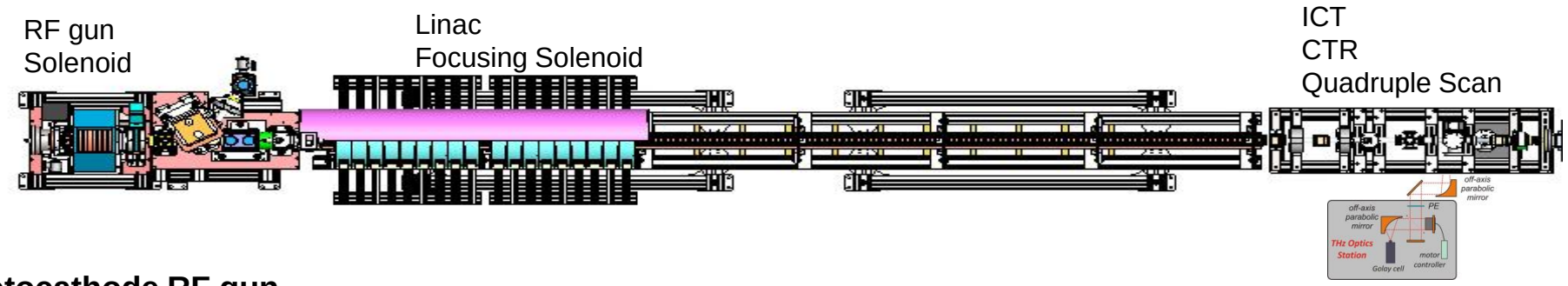

Photocathode RF gun
- S-band 1.6-cell copper cavity
- Cu photocathode (QE:10^{-6}~10^{-5})
- Emittance compensation solenoid

Laser system
- IR(800 nm) & UV (266 nm) sources
- Beam shaping elements

RFSystem
- Thalas 35MW pulsed klystron
- Power devider and Phase shifter

Beam Diagnostic Tools
- ICT, Faraday cup, YAG screen, multislit,
- spectrometer, quadruple scan, CTR…

Linac
- S-band, 5.2 m, 156-cell copper, constant gradient
- Focusing Solenoid

- Beam emittance and brightness
- **Electron Source**
- Electron guns
- Bunch compressor
- Beam diagnostics

Thermionic Emission

Energy Level Diagram for Electrons Near the Surface of Metal

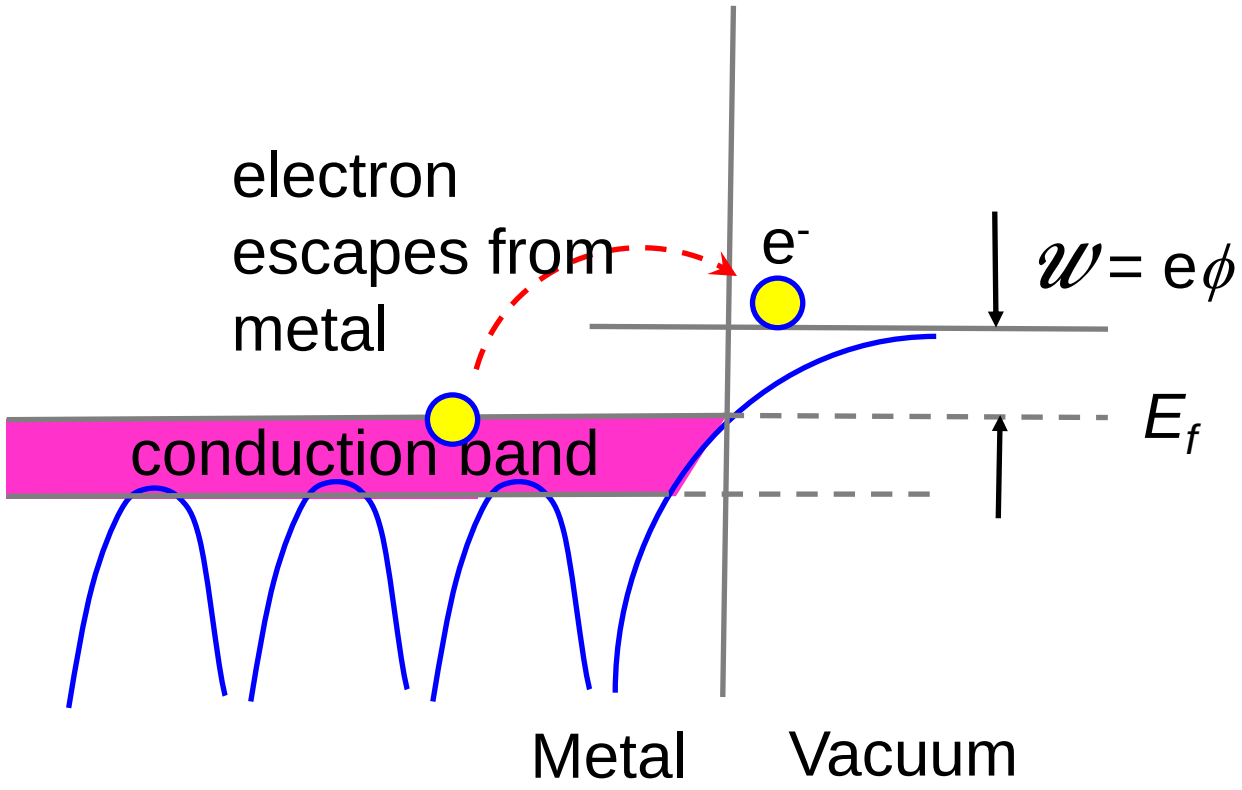

- Work function *W* depends on cathode material and operation temperature
- Common thermionic cathode materials are W (Tungsten), LaB_6, Ba etc..
- For W (Tungsten), *W* = 4.6 eV; Cu, *W* = *4.3 eV* and for Ba, *W*=1.8 eV.
- Richardson-Dushmann equation:

$$J_{th} = A_0 T^2 e^{-\frac{W}{kT}}$$

$$A_0 = \frac{4\pi emk^2}{h^3} = 120 A/cm^2 K^2$$

Thermionic Emission of Various Cathode Materials

	A ($Acm^{-2}K^{-2}$)	ϕ (eV)	Melting Temp. (°C)
Ba	60	2.11	720
Cesium	160	1.81	28
Ta	60	4.12	2850
W	60	4.54	3370
Thoriated W	3	2.63	--
Mixed oxide	0.01	~1	--
Cs/O/W	0.003	0.72	--
LaB_6	29	2.66	2210

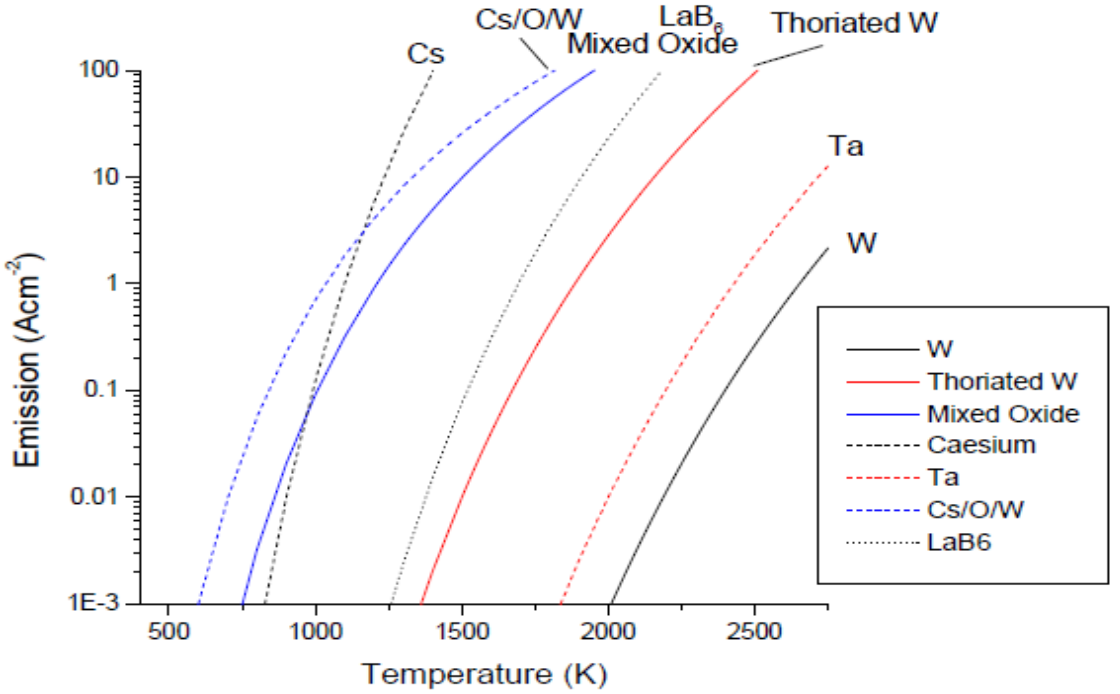

Thermionic Cathode

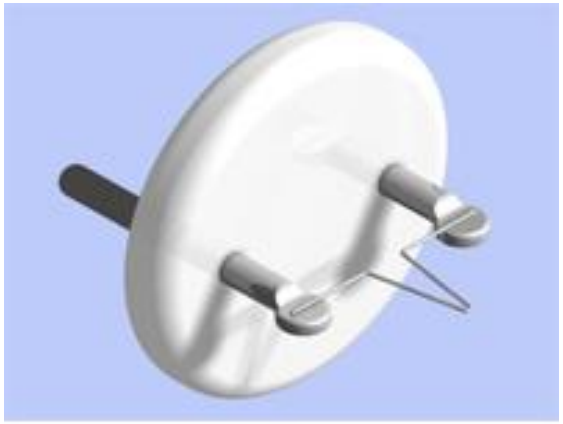

tungsten filament for electron microscope

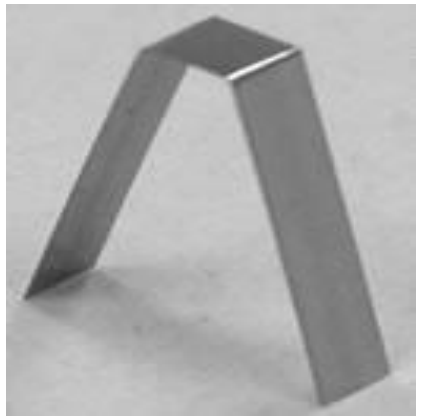

filament cathode for e-beam welder

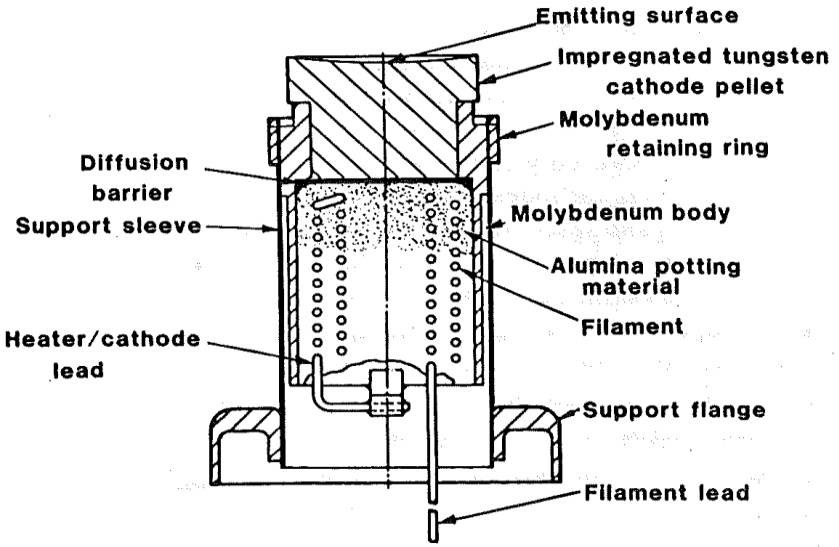

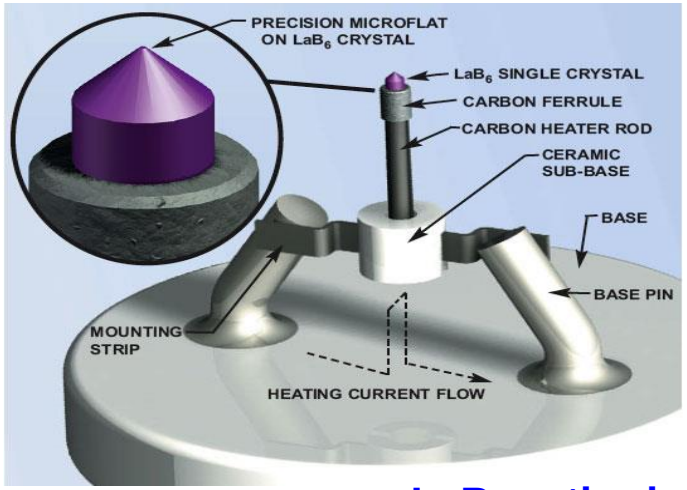

LaB_6 cathode for electron microscope

a typical type B dispenser cathode for linac system

Emittance of a Thermionic Cathode

Assume a thermonic cathode of radius r_s is operating at temperature T, RMS velocity spread is

$$\tilde{v}_x = \tilde{v}_y = \left(\frac{k_B T}{m}\right)^{1/2}$$

RMS thermal velocity spread is related to rms beam divergence as

$$\tilde{x}' = \tilde{v}_x / v_0$$

On the other hand, *RMS* beam size is $\tilde{x} = \tilde{y} = r_s / 2$, since

$$\tilde{x} = \frac{\tilde{r}}{\sqrt{2}} = \frac{1}{\sqrt{2}}\left[\frac{2\pi n_0 \int_0^a r^3 dr}{2\pi n_0 \int_0^a r dr}\right]^{1/2}$$

Maxwellian velocity distribution

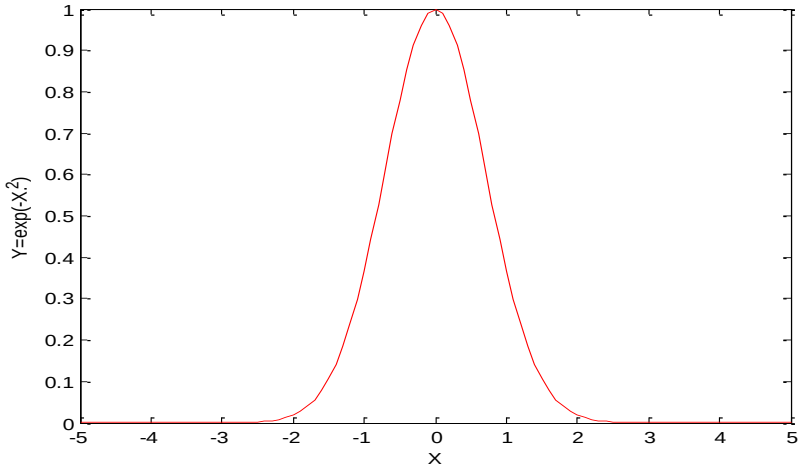

$$f(v_x, v_y, v_z) = f_0 \exp\left[-\frac{m\left(v_x^2 + v_y^2 + v_z^2\right)}{2k_B T}\right]$$

$$\tilde{\varepsilon}_{x,y} = \tilde{x}\tilde{x}' = 2r_s \frac{\left(\frac{k_B T}{m}\right)^{1/2}}{v_0} \Rightarrow \tilde{\varepsilon}_n = 2r_s \left(\frac{k_B T}{m v_0^2}\right)^{1/2}$$

low temperature, small cathode ➔ low emittance

Planar Diode with Space Charge : Child-Langmuir Law

$$\begin{cases} \nabla^2\phi = \dfrac{d^2\phi}{dx^2} = -\dfrac{\rho}{\varepsilon_0} \\ J_x = \rho\dot{x} = const \\ \dfrac{m}{2}\dot{x}^2 - e\phi(x) = 0 \end{cases}$$

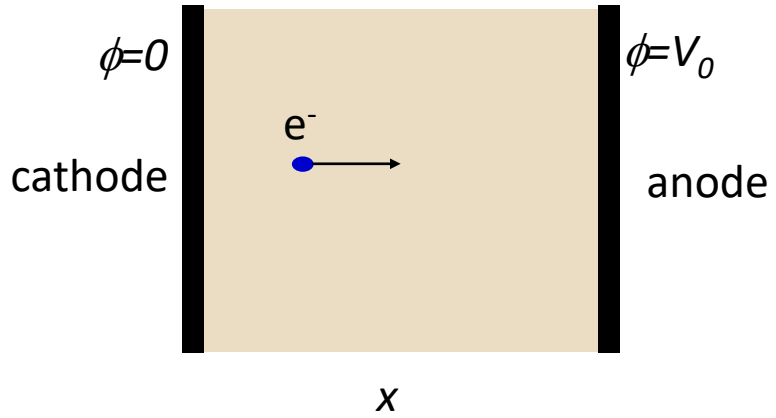

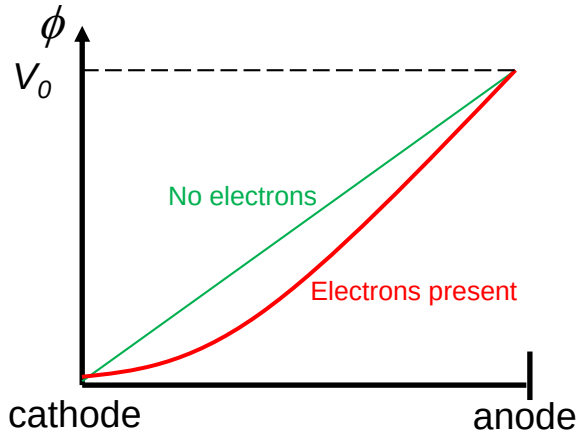

$$\Rightarrow \frac{d^2\phi}{dx^2} = \frac{J}{\varepsilon_0(2e/m)^{1/2}}\frac{1}{(\phi)^{1/2}}$$

$$\Rightarrow \left(\frac{d\phi}{dx}\right)^2 = \frac{4J}{\varepsilon_0(2e/m)^{1/2}}\phi^{1/2} + C$$

*C=0 under the boundary conditions: ϕ=0 and dϕ/dx=0 at x=0; the condition dϕ/dx=0 at x=0 implies that the special case **electric field at cathode surface is null** (a steady state solution).*

$$\Rightarrow \frac{4}{3}\phi^{3/4} = 2\left(\frac{J}{\varepsilon_0}\right)^{1/2}\left(\frac{2e}{m}\right)^{-1/4}x$$

$$\Rightarrow \phi(x) = V_0\left(\frac{x}{d}\right)^{4/3} \text{ with}$$

Child-Langmuir law

$$J = \frac{4}{9}\varepsilon_0\left(\frac{2e}{m}\right)^{1/2}\frac{V_0^{3/2}}{d^2}$$

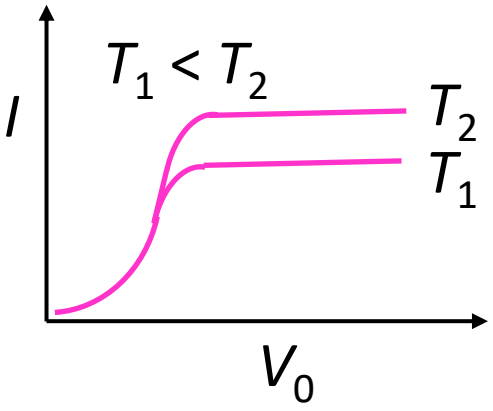

Schottky Effect

x_m and the potential at x_m can be found as:

$$x_m = \left(\frac{e}{16\pi\varepsilon_0 E}\right)^{1/2}$$

$$\phi' = -\frac{e^2}{16\pi\varepsilon_0 x_m} - eEx_m$$

or $$\phi' = -W' = -e\left(\frac{eE}{4\pi\varepsilon_0}\right)^{1/2}$$

$$J_e = A_0 T^2 e^{-(W-\Delta W)/kT} = J_{th} e^{\Delta W/kT}$$

$$J_e = J_{th} \exp\left[\frac{e(eE/4\pi\varepsilon_0)^{1/2}}{kT}\right]$$

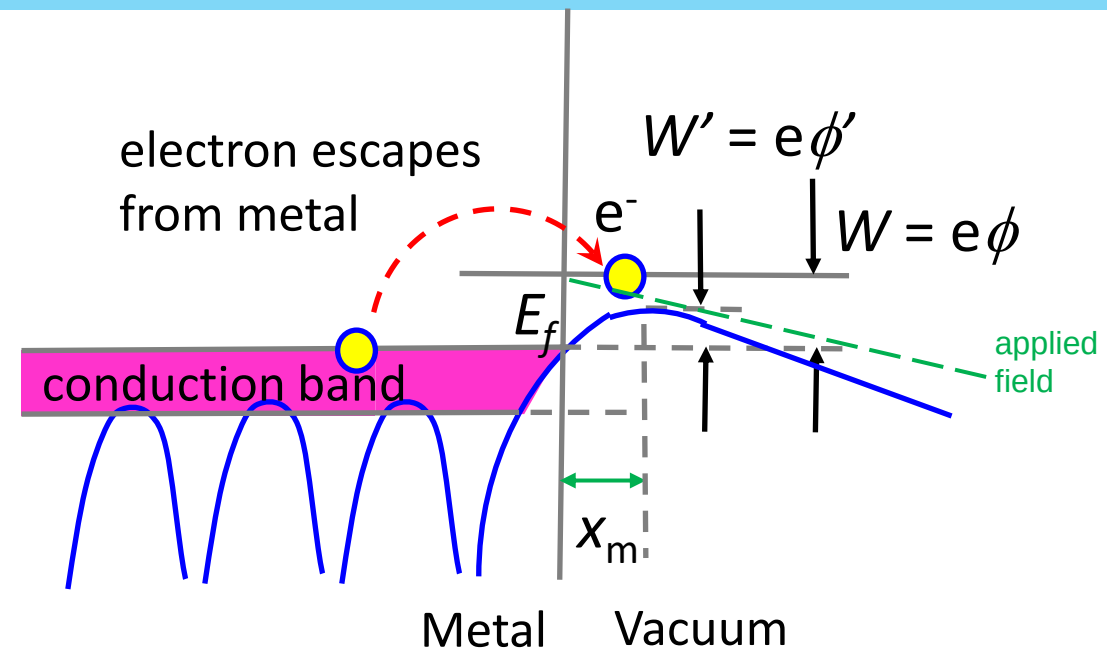

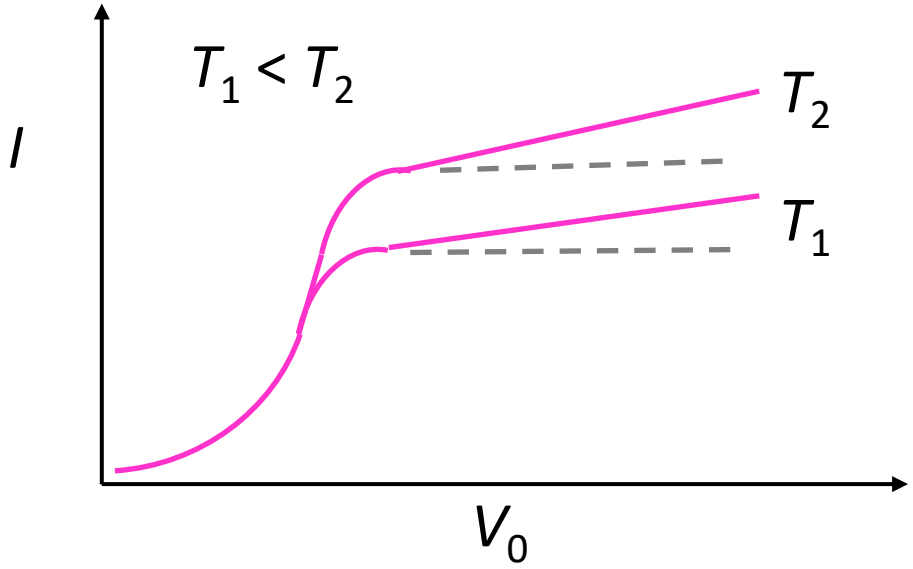

Field Emission and Dark Current

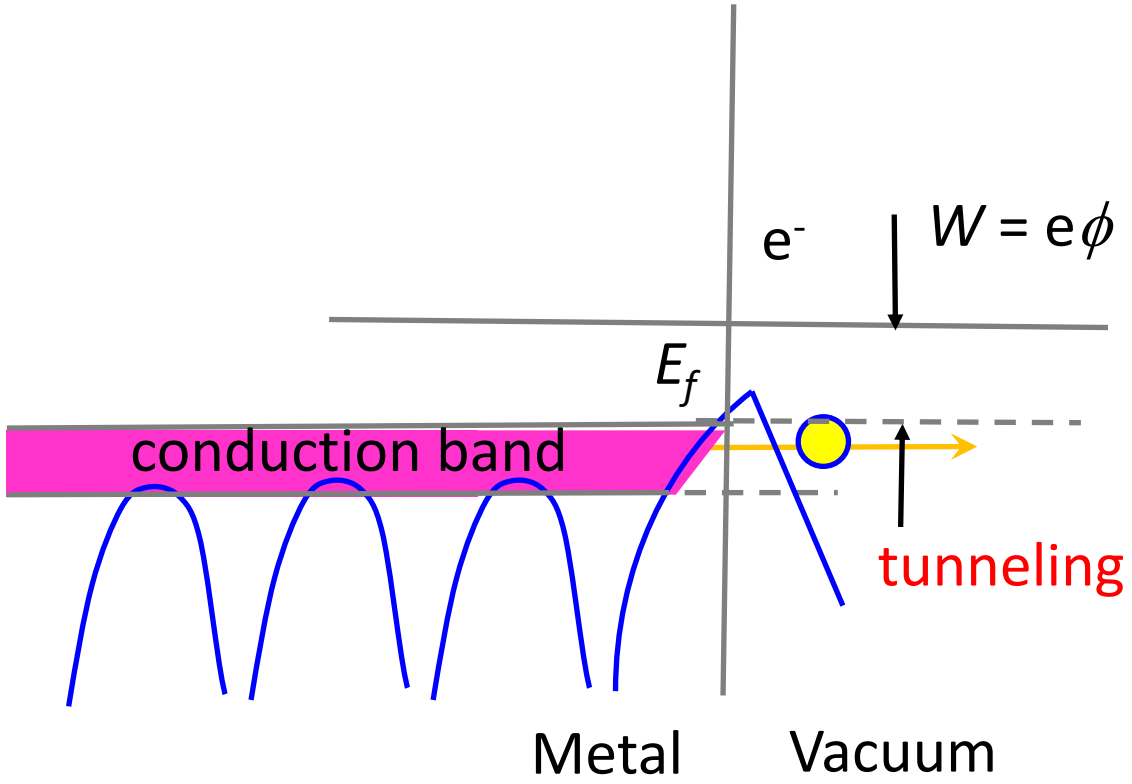

$$J_f = CE^2 e^{-D/E}$$

field emission current density

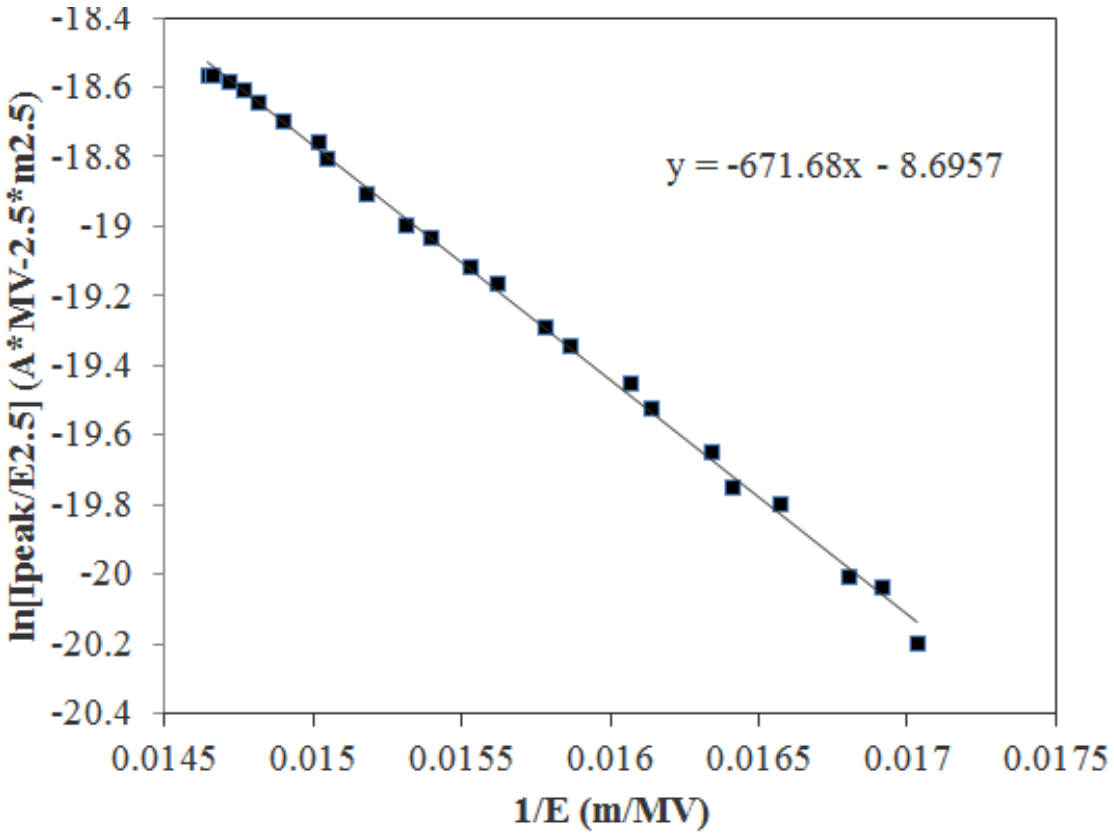

Fowler-Nordheim plot in dark current measurement

Effect of Surface Roughness on Emission

- Micro-protrusions and surface contaminants can effectively enhance the field at the emitting surfaces.
- Field enhancement due to surface roughness, non-metallic inclusions in cracks or grain boundaries etc. has negligible effect on QE for planar geometries.
- Normalized emittance varies as the effective work function and the field distribution change from the peak to the valley of the rough cathode surface.
- Non-uniform charge density at/near the cathode surface.

distribution of field lines in the vicinity of one of the protrusions

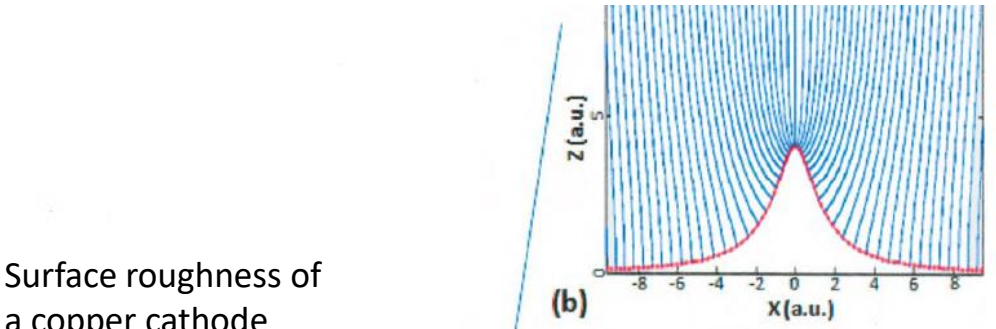

Surface roughness of a copper cathode

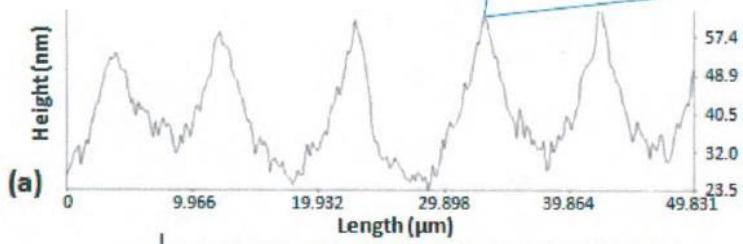

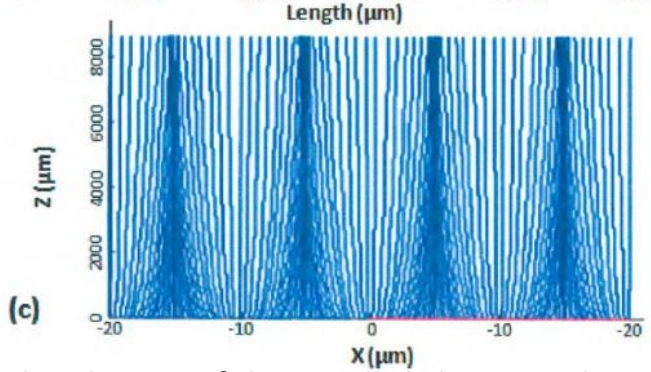

distribution of the emitted charge in the vicinity and a few mm away from the cathode

T. Rao and D.H. Dowell, “An Engineering Guide to Photoinjectors” (2013)

Photoelectric Emission

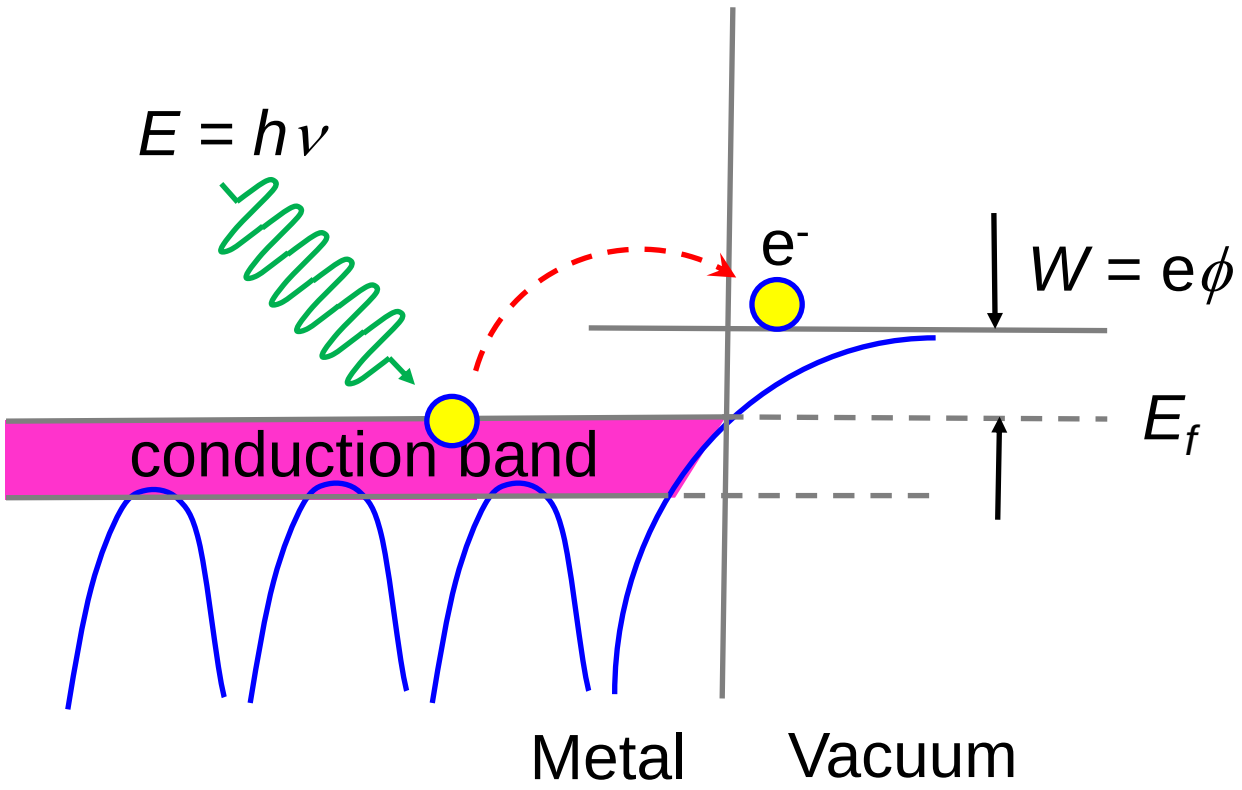

T. Rao and D.H. Dowell, "An Engineering Guide to Photoinjectors" (2013)

Quantum efficiency:

$$QE = \frac{n_e}{n_p}$$

n_p is the number of incident (absorbed) photons

Since laser energy is a measurable quantity, QE can be expressed as

$$QE = \frac{h\nu[eV]}{E_{laser}[J]} \cdot q[C]$$

QE is a function of photon energy.

$$QE(\nu) \propto (h\nu - \phi)^2$$

Intrinsic emittance of metallic photo-cathode:

$$\varepsilon_n = \sigma_x \sqrt{\frac{h\nu - \phi}{3mc^2}}$$

QE of common metal photo-cathodes

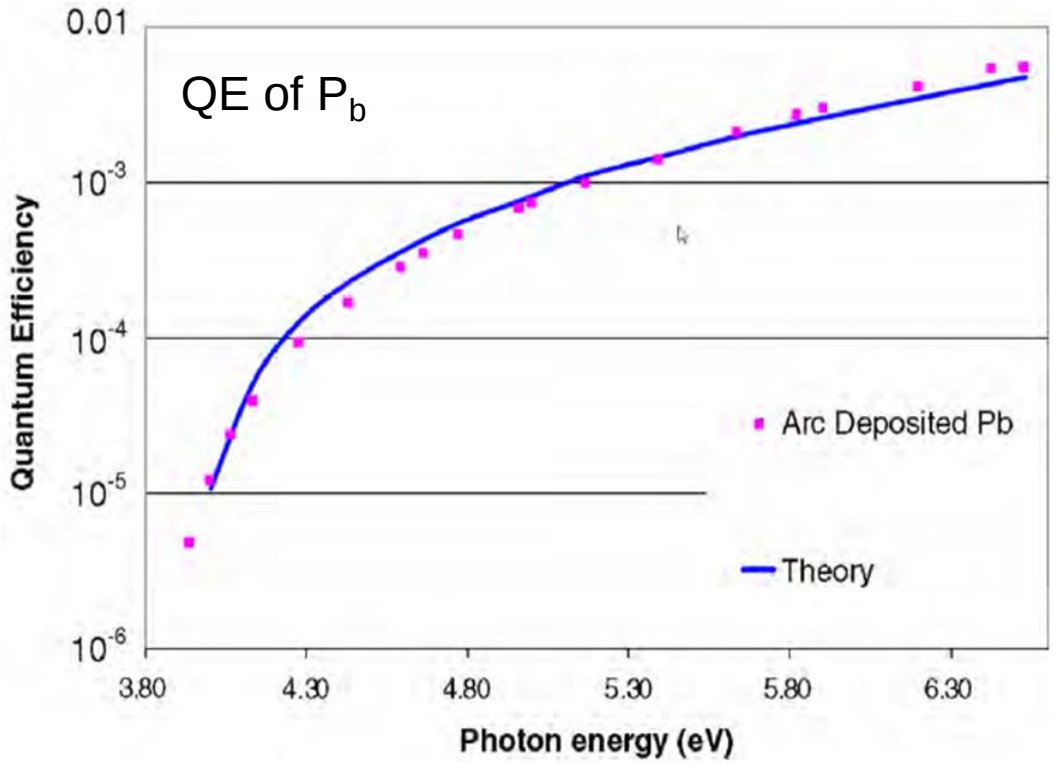

Metal @ Electric Field	Wavelength [nm]	QE [%]
Copper @ 100 MV m^{-1}	266	0.014
Magnesium @ 100 MV m^{-1}	266	0.62
Niobium @ 2 MV m^{-1}	266	~0.001
Lead @ 2 MV m^{-1}	248	0.016

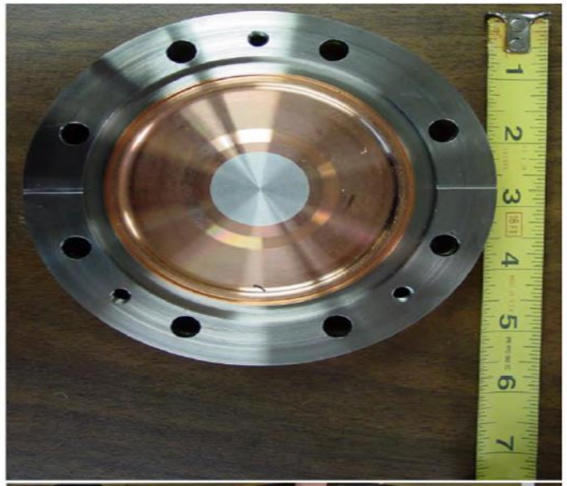

Mg cathode

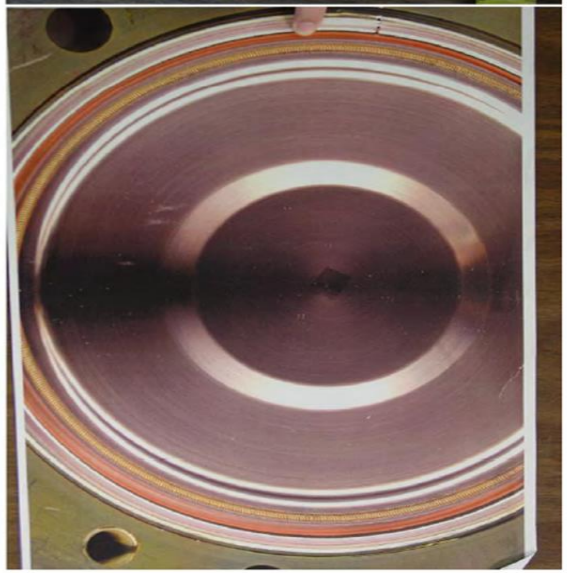

Cu cathode

Common Photo-cathodes

- **Metal: Cu**
  - <~sub-picosecond pulse capability
  - minimally reactive; requires ~ 10^{-8} Torr pressure
  - low QE ~ 10^{-5}~10^{-4}
  - requires UV light
  - for nC, 120 Hz reptition rate, ~ 2 W of IR required

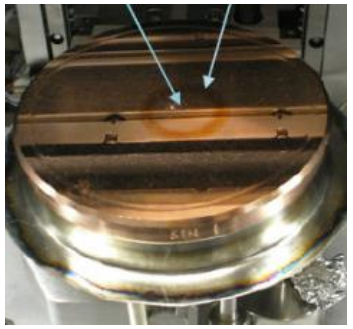

- **PEA Semiconductor: Cesium Telluride Cs_2Te**
  - <~ps pulse capability
  - relatively robust and un-reactive (operates at ~ 10^{-9} Torr)
  - Successfully use in NC RF and SRF guns
  - high QE > 5%
  - photo-emits in the UV ~250 nm

- **NEA Semiconductor: Gallium Arsenide GaAs**
  - tens of ps pulse capability with phonon damping
  - reactive; requires UHV <~ 10^{-10} Torr pressure
  - high QE (typ. 10%)
  - Photo-emits already in the NIR,
  - for nC, 1 MHz, ~50 mW of IR required
  - operated only in DC guns at the moment

In general :
- Metal cathodes are more robust but show much lower QE.
- Semiconductor cathodes have high QE. but short life time.

- Beam emittance and brightness
- Electron Source
- **Electron guns**
- Bunch compressor
- Beam diagnostics

DC and RF Acceleration

DC acceleration

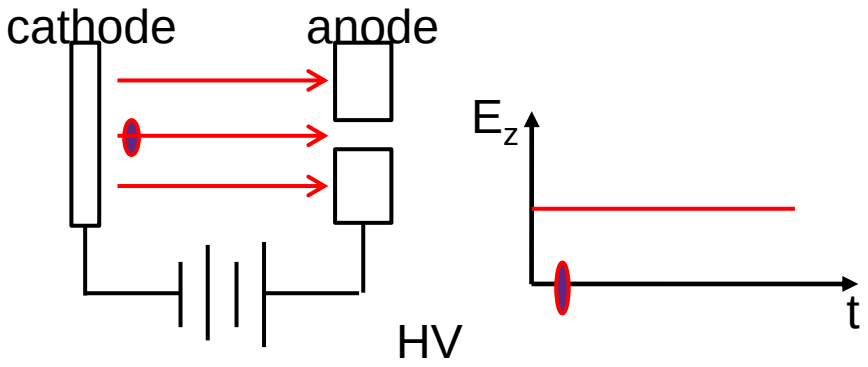

RF acceleration

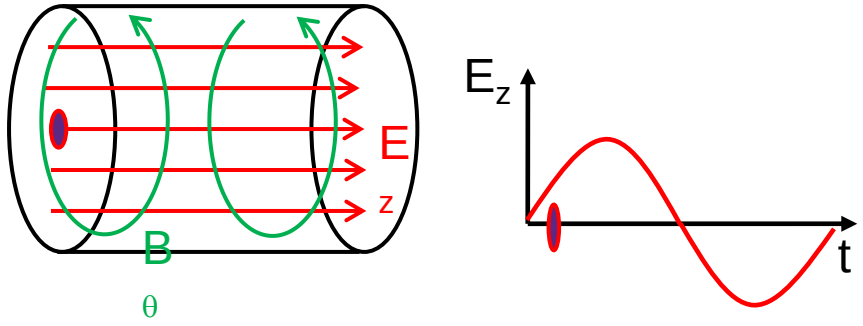

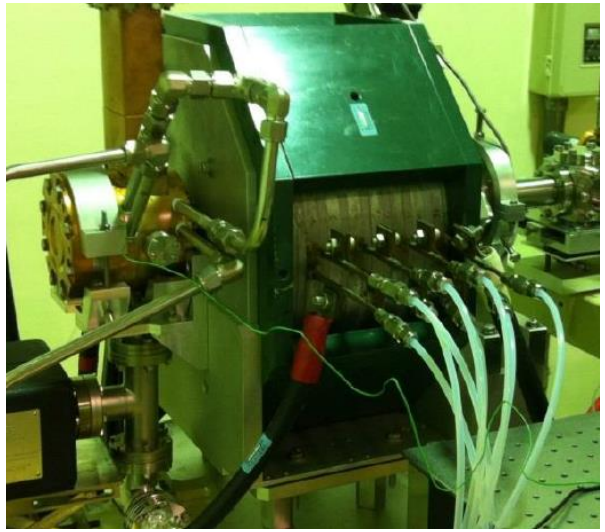

Electron Gun with Pierce Electrode

- Electrostatic repulsion forces between electrons tend to diverge the beam.
- The required current density of electron beam is usually far greater than the available emission density of cathode.
- Optimum angle of focusing electrode for a parallel beam is referred to as 'Pierce electrodes'.
- Defocusing effect of *anode aperture* has to be considered.

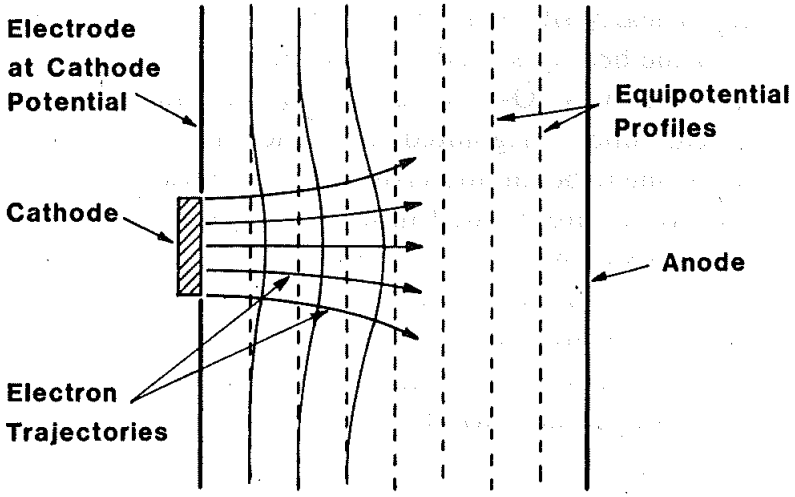

a simple parallel-plate diode

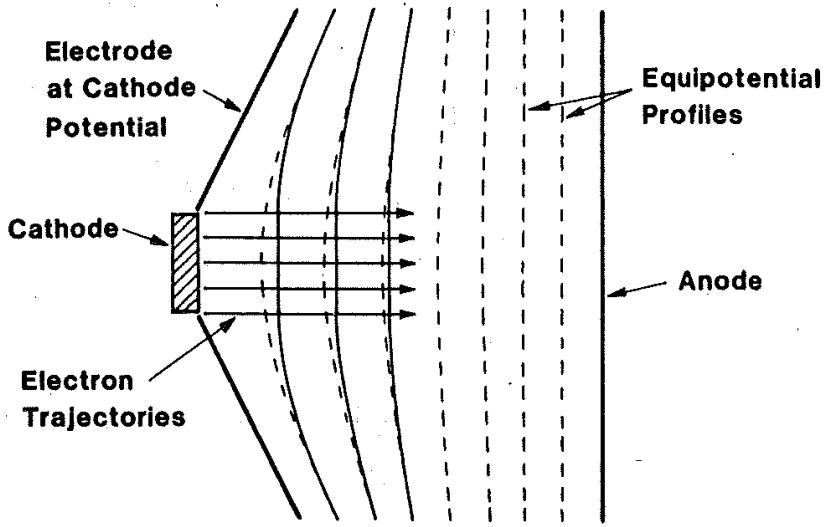

a diode gun with Pierce electrodes (Pierce gun)

Cavity Modes in a Pillbox

$$E_z = E_0 J_m(k_{mn} r)\cos(m\theta)\cos(k_l z)e^{j\omega t}$$

$$E_r = -\frac{jk_l}{k_{mn}} E_0 J_m{}'(k_{mn} r)\cos(m\theta)\sin(k_l z)e^{j\omega t}$$

$$E_\theta = -\frac{k_l m}{k_{mn}^2 r} E_0 J_m(k_{mn} r)\sin(m\theta)\sin(k_l z)\, e^{j\omega t}$$

$$B_r = \frac{\omega m}{k_{mn}^2 cr} E_0 J_m(k_{mn} r)\sin(m\theta)\cos(k_l z)\, e^{j\omega t}$$

$$B_\theta = \frac{j\omega}{k_{mn} c} E_0 J_m{}'(k_{mn} r)\cos(m\theta)\cos(k_l z)\, e^{j\omega t}$$

$$B_z = 0$$

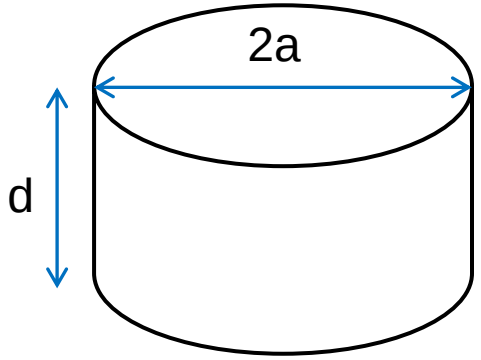

Where $k_l = l\pi/d\,, l = 0,1,2,\ldots$

$k_{mn} = x_{mn}/a$

The n[th] zero of $J_{mn}(x)$

Resonant frequency : $f_{mnl} = \frac{c}{2\pi}\sqrt{\left(\frac{l\pi}{d}\right)^2 + \left(\frac{x_{mn}}{a}\right)^2}$

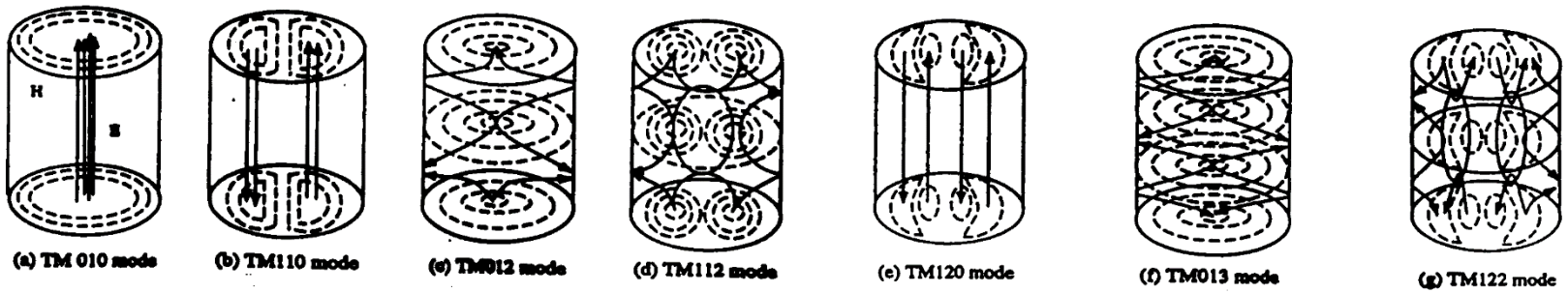

Cavity Mode for Particles Acceleration

The lowest-frequency TM mode is TM_{010} with cell length = $\lambda/2$.

$$E_z = E_0 J_0(k_{01} r) e^{j\omega t}$$

$$E_r = 0$$

$$E_\theta = 0$$

$$B_\theta = \frac{j\omega}{k_{01} c} E_0 J_0'(k_{01} r) e^{j\omega t}$$

$$B_r = 0$$

$$B_z = 0$$

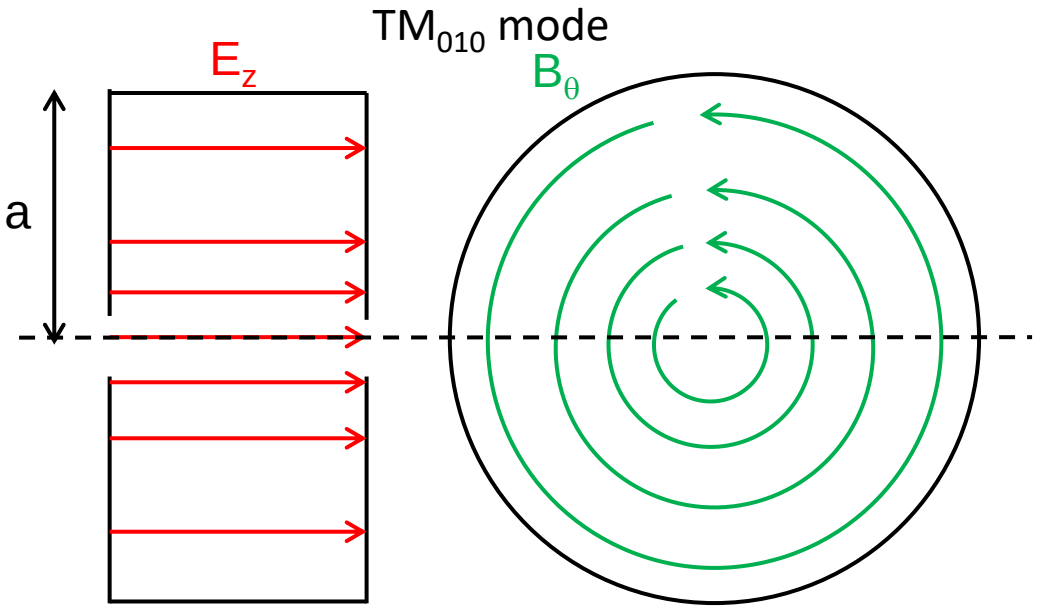

TM010 resonance frequency : $f_{01} = \frac{2.405}{2\pi}\frac{c}{a}$

Example : *a = 3.825 cm,* $f_{01} = 3\ GHz$

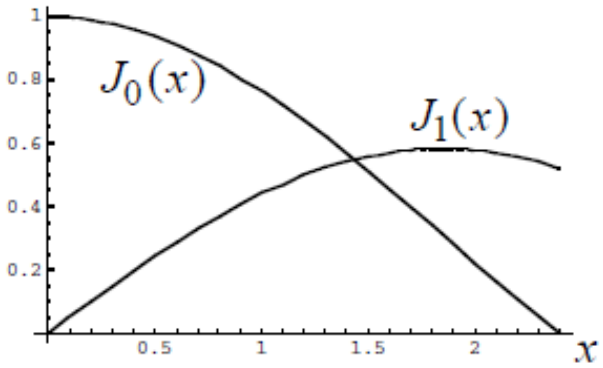

RF Gun

- RF guns are used to produce high peak current electron beams
- Usually operate at low repetition and GHz frequencies range (typically 3GHz).
- The cavity structure is usually n+1/2cell(n=1,3…)
- Standing wave structure, TM mode to accelerate the beam
- The cathode is placed in the half cell (max field)
- The radio frequency gun accelerates the photoelectrons emitted at the photocathode surface, up to a relativistic speed ***in a time shorter than the RF period.***

The BNL/SLAC/UCLA photocathode RF Gun

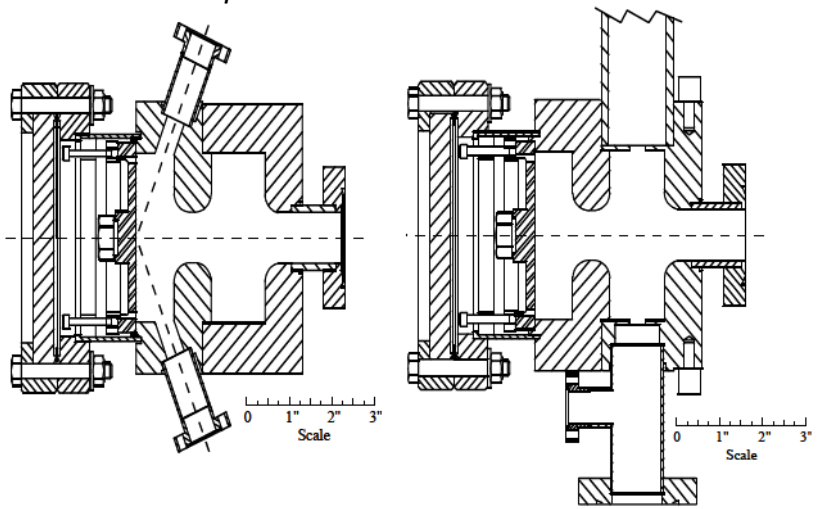

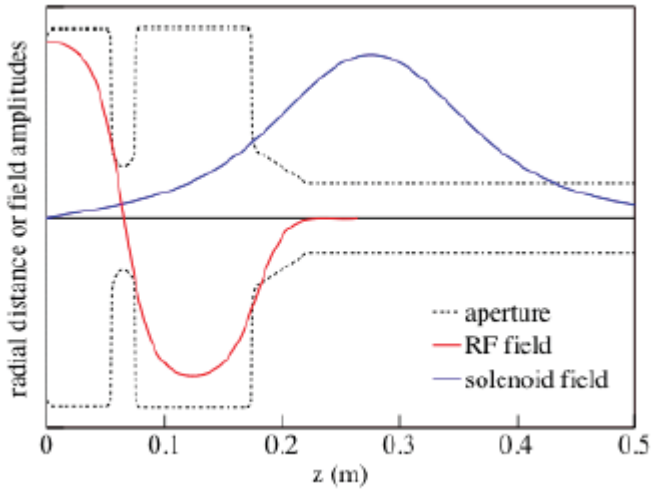

Gun Cavity

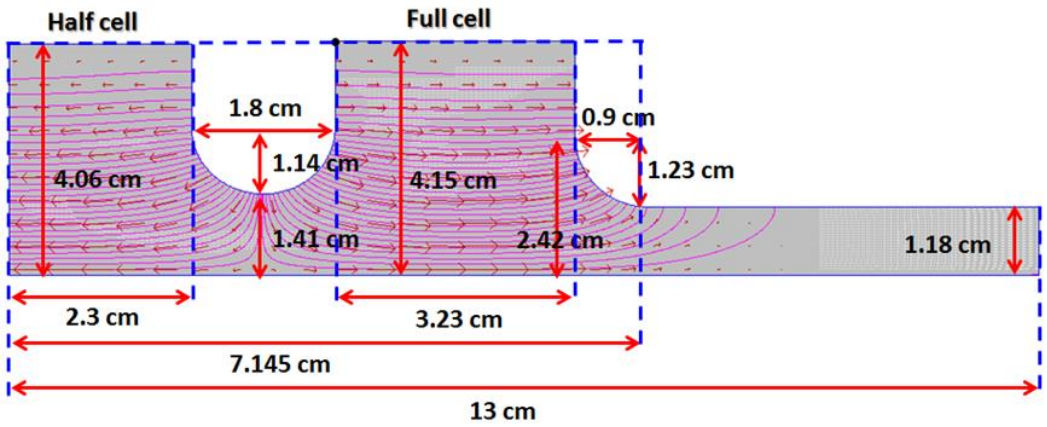

- Coupled cavity mode is π-mode.
- The cavity cells are on-axis coupled through apertures, coupling strength depends on diameter of apertures.

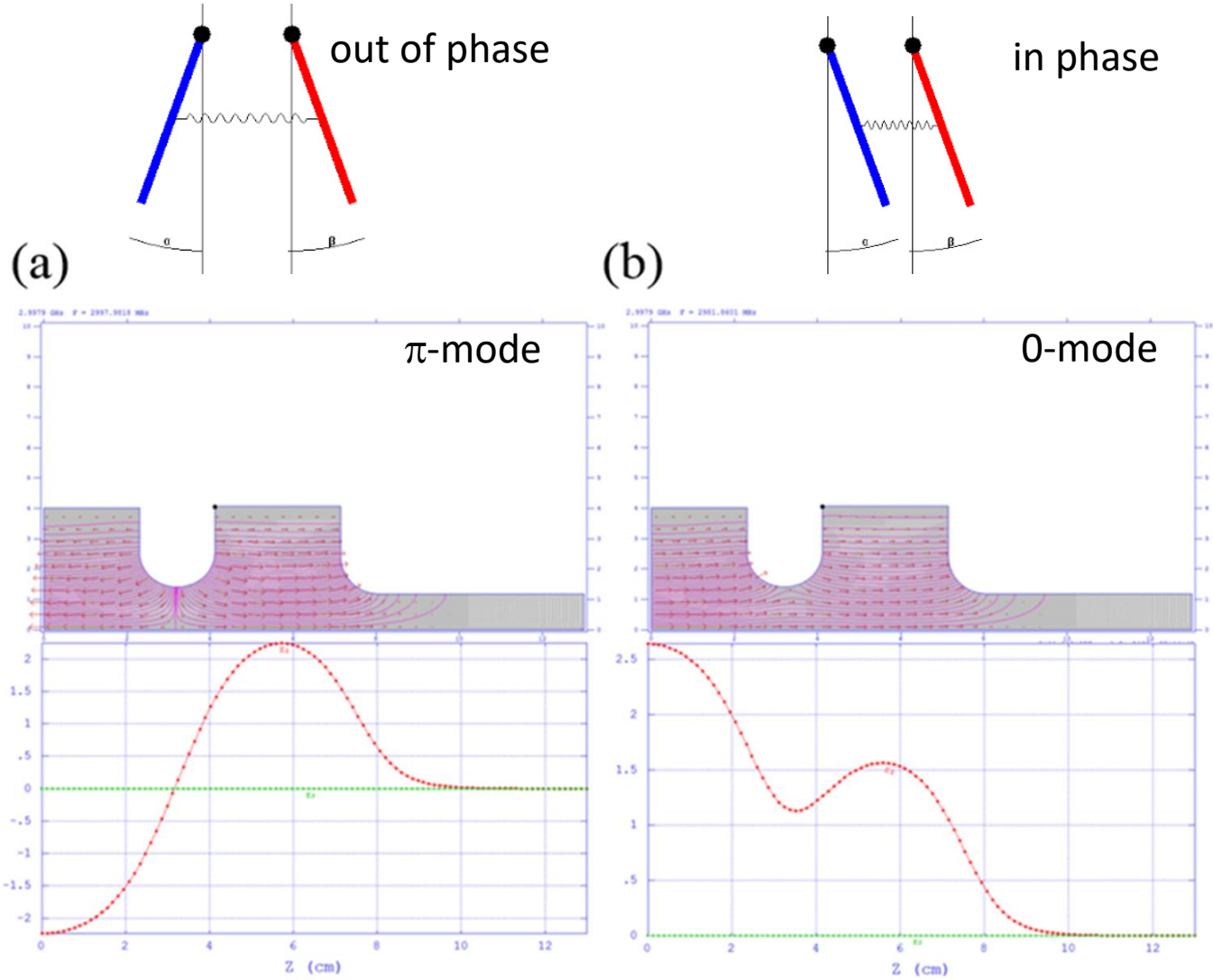

* balance of field amplitude for efficient acceleration

Thermionic Cathode Radio Frequency Electron Gun

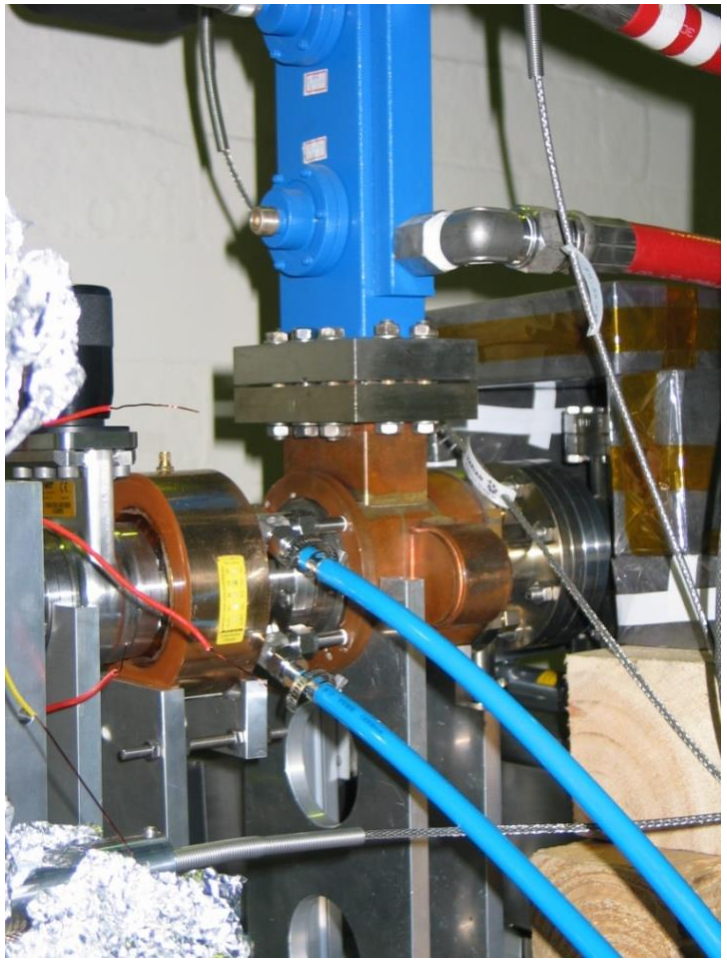

Thermionic Cathode RF Gun

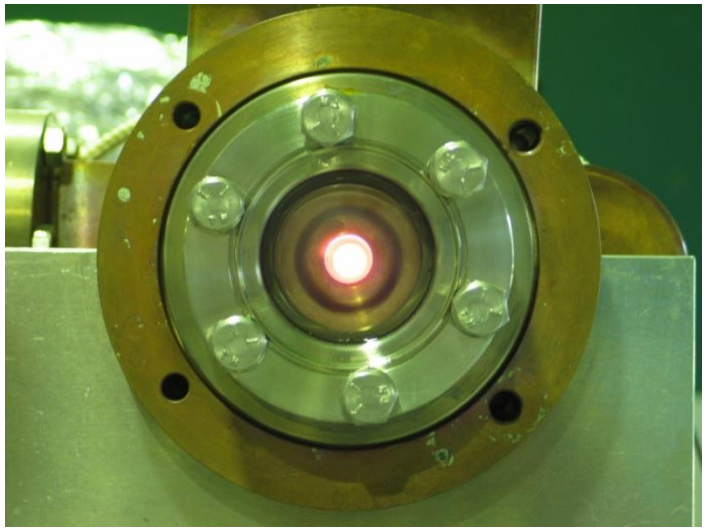

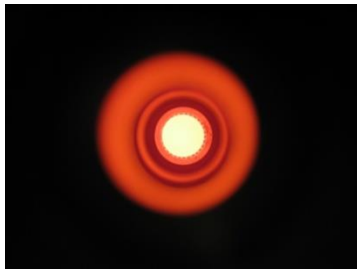

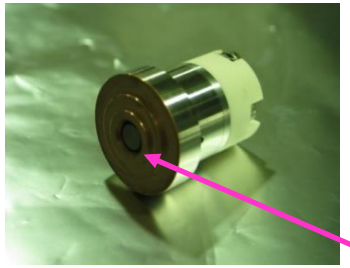

cathode operating
at 1100 °C during activation

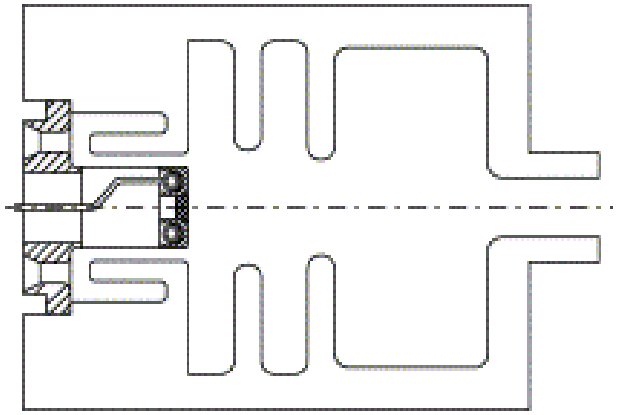

MAX-Lab π/2-mode thermionic rf gun with rf choke

cathode assembly with heat barrier

Cornell Photocathode DC Gun

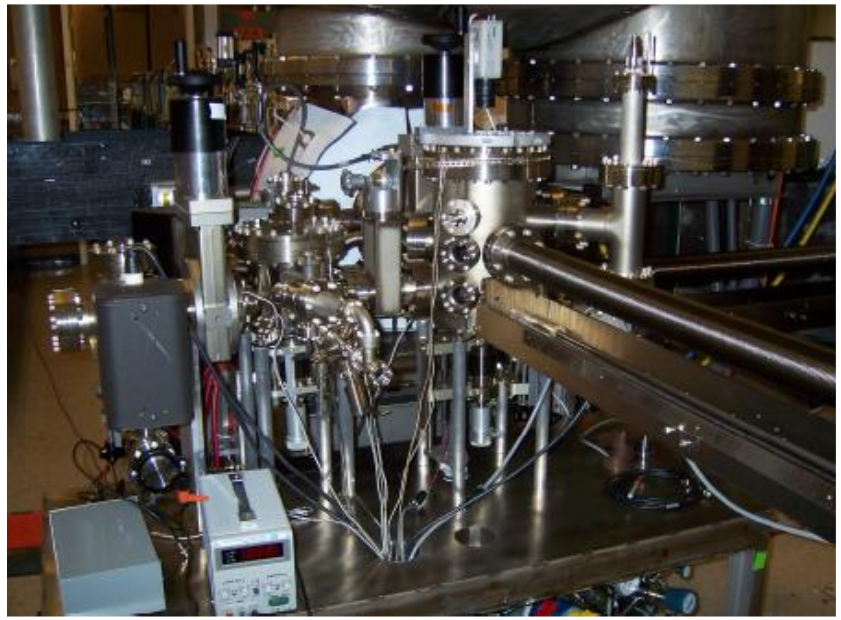

Cornell DC gun	
Gun exit energy	0.35 MeV
repetition rate	1300 MHz
rms emittance	0.5 mm at 80 pC
Average current	65 mA (at 50 pC)

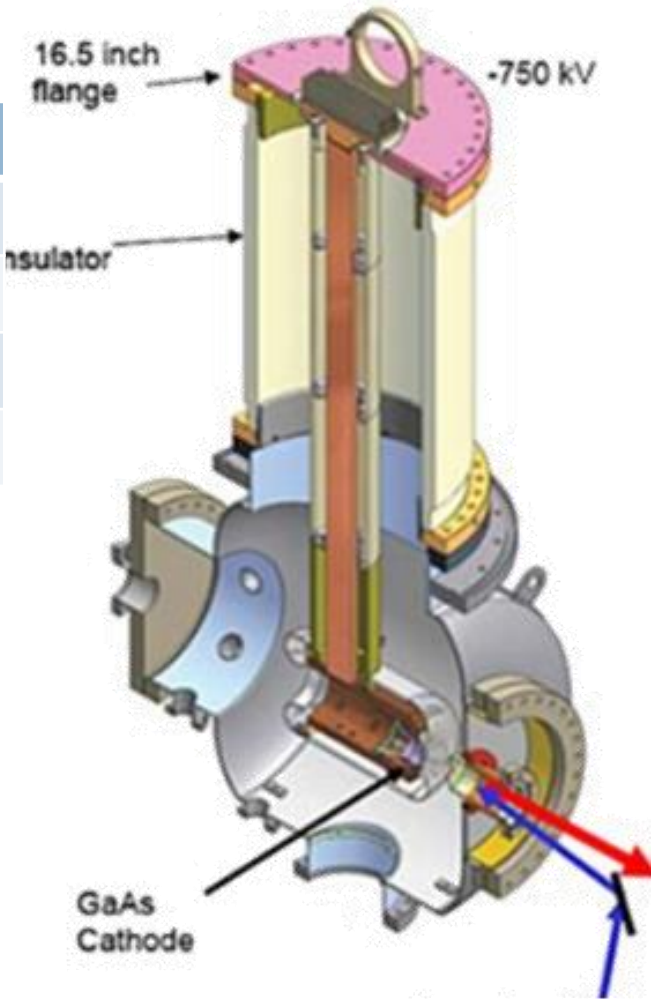

Cornell DC gun

- High QE cathode to minimize laser heating
- GaAs cathode, require ultra high vacuum at 10^{-12} mbar
- Smooth electrode surfaces to minimize field emission
- Need reliable HVDC power supply and insulator design
- Low beam energy, need more complicated injector design.
- Capability to provide sub-μm, few hundred pC beam.
- Stable operation at ~ 400 kV

K. Smolenski et al., "Design and Performance of the Cornell ERL DC Photoemission Gun" AIP Conference Proceedings 1149, 1077–1083 (2009)

LCLS S-BAND NC RF Gun

The LCLS S-Band Gun :

- Dual RF Feeds – to eliminate the dipole modes
- Racetrack shape of the full cell – to minimize the quadruple mode
- Elliptical disk iris shape : to reduce the surface field.
- Z-coupling of RF feeds : to reduce the pulsed heating
- Increase the mode separation : to reduce the 0 mode amplitude

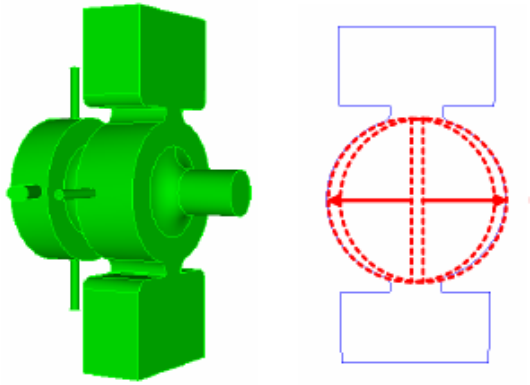

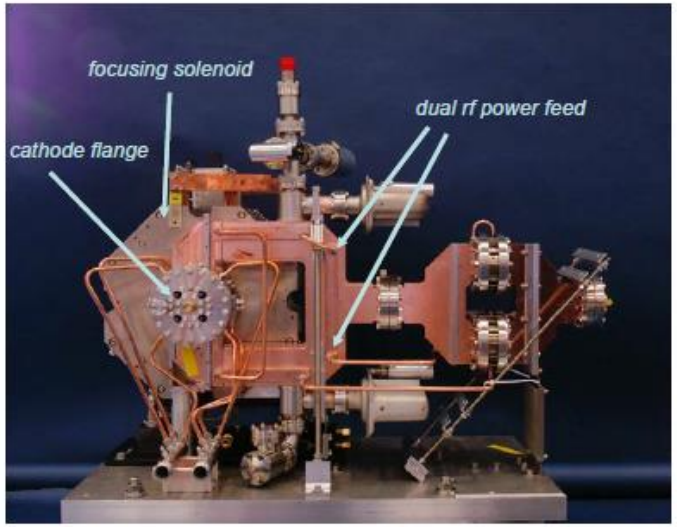

	BNL/SLAC/UCLA Gun III	LCLS Gun
cathode field	120MV/m	140MV/m
rf feed	single w/compensation port	dual feed
cavity shape	circular	racetrack
0-π mode separation	3.4MHz	15MHz
repetition rate	10Hz	120Hz
peak quadrupole field	4 mrad/mm	0.1 mrad/mm
RF tuners	plunger/stub	deformation
cathode	copper or Mg	copper
rf coupling	theta (azimuth)	z (longitudinal)
β-coupling	1.3	2.0
laser incidence	grazing or normal	grazing or normal

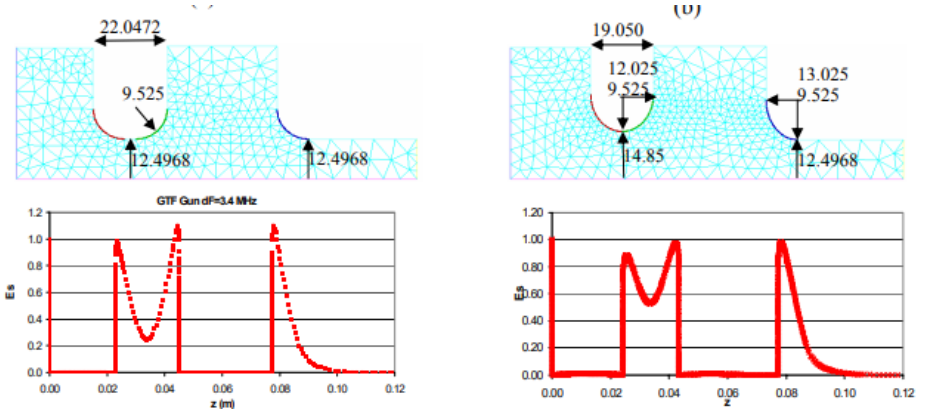

C.Limborg et al.,“RF Design of the LCLS Gun”, SLAC-TN-10-094, 2005

The PITZ Gun

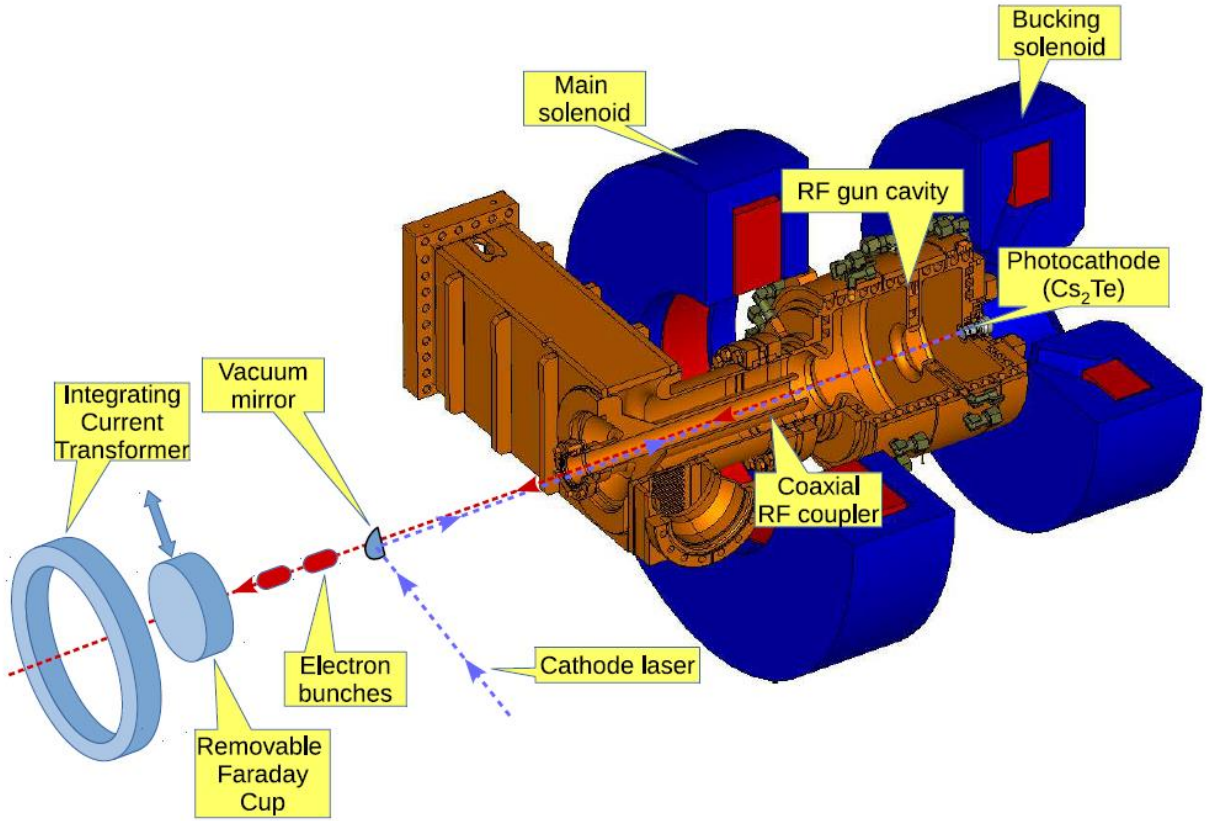

- operating frequency @ 1300 MHz
- Cs_2Te cathode delivers 0.001 – 4 nC bunch charge
- Beam mean energy 6.5 MeV
- Number of electron pulses in bunch train < 800
- Macropulse repetition rate 10 Hz
- Bunch rep.-rate 1kHz
- Average beam current 32 μA max.
- Optimized emittance < 0.9 μm

Igor Isaev, “Stability and Performance Studies of the PITZ Photoelectron Gun”, University of Hamburg dissertation (2017)

The PITZ Gun

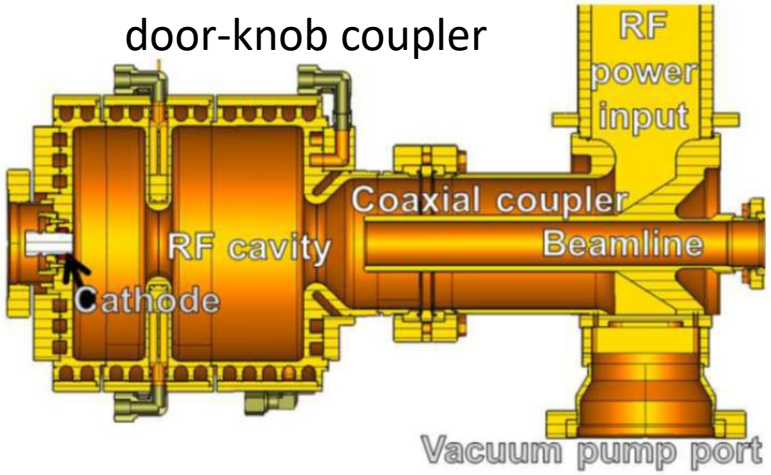

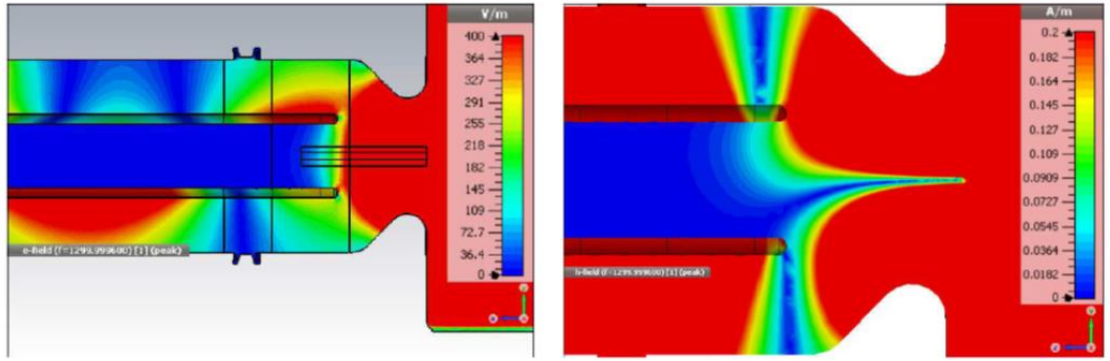

(a) E RF field distribution (b) H RF field distribution

CLARA S-band photocathode rf gun

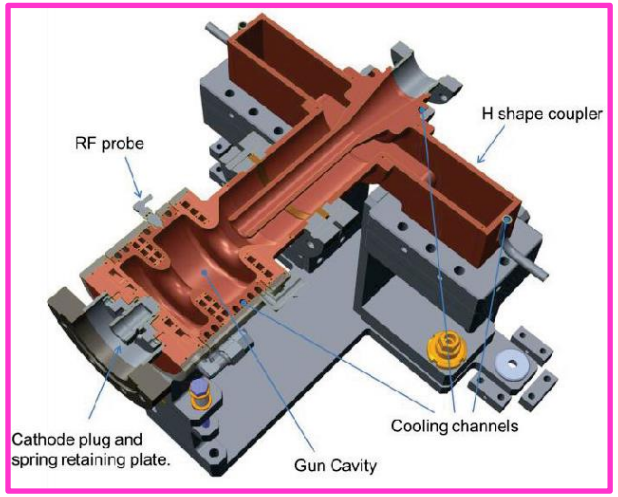

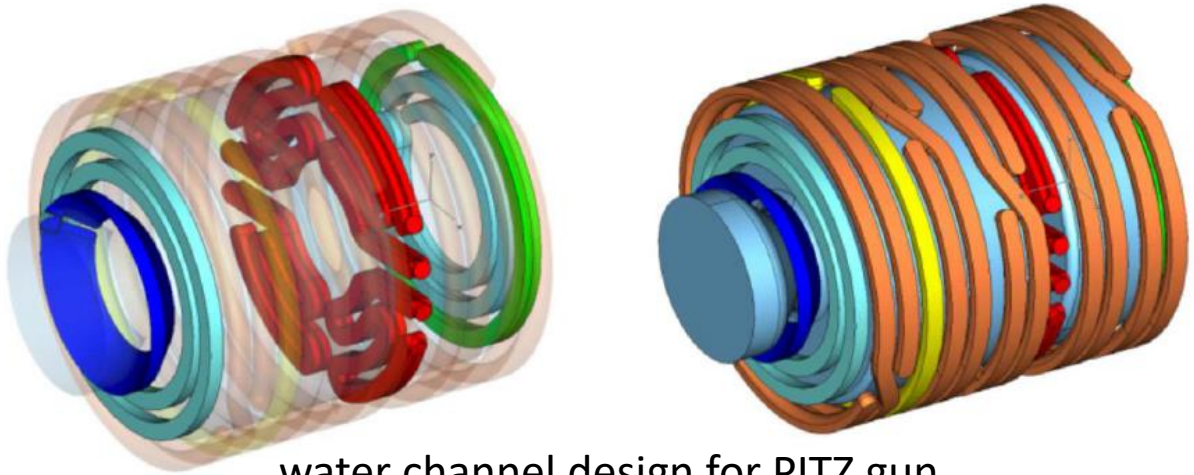

water channel design for PITZ gun

Igor Isaev, “Stability and Performance Studies of the PITZ Photoelectron Gun”, University of Hamburg dissertation (2017)

LBNL CW Photocathode RF Gun

- At the VHF frequency, the cavity structure is large enough to withstand the heat load at a level that conventional cooling techniques can be used to run in CW mode.
- The long wavelength allows for large apertures and thus for high vacuum conductivity.

Total length [m]	0.35
Cavity internal diameter [m]	0.694
Accelerating gap [mm]	40
Frequency [MHz]	187
Q_0 (ideal copper)	30877
Gap voltage [MV]	0.75
Electric field at the cathode [MV/m]	19.5
Peak surface electric field [MV/m]	24.1
Stored energy [J]	2.3
Shunt impedance [MΩ]	6.5
RF power for 0.75 MV at Q_0 [kW]	87.5
Peak wall power density at 0.75 MV [W/cm^2]	25.0

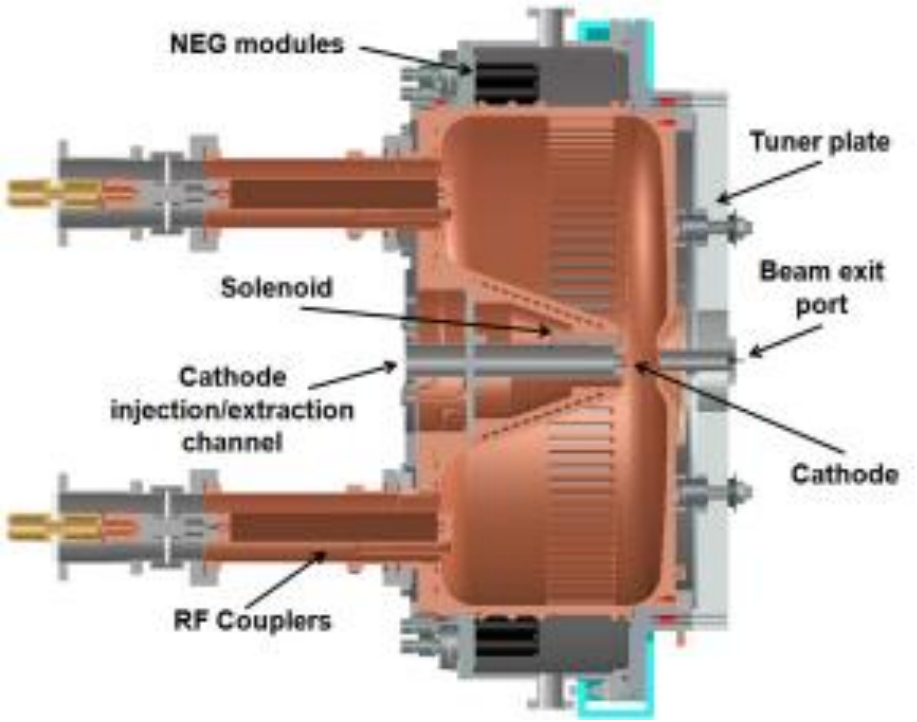

186 MHz LBNL CW photo-cathode rf gun

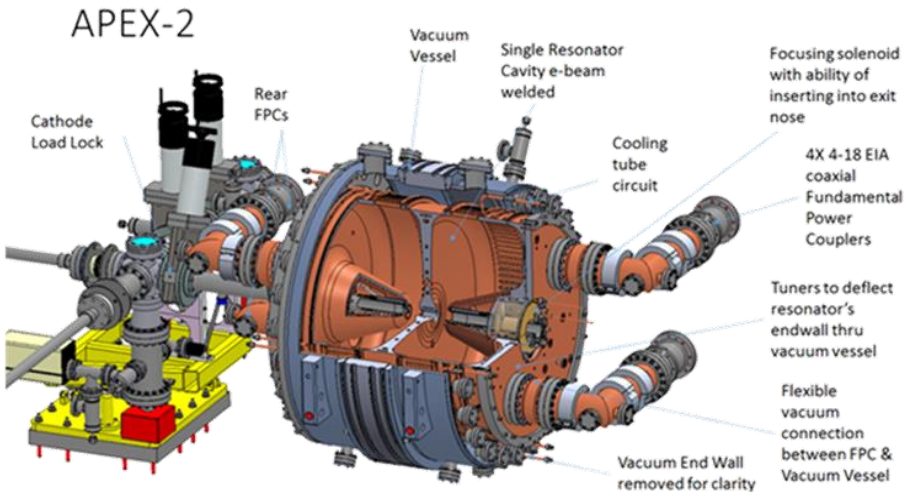

2-cell cavity operating at 162.5 MHz

F. Sannibale et al., STATUS OF THE LBNL NORMAL-CONDUCTING CW VHF ELECTRON PHOTO-GUN, WEBP36, Proceedings of FEL201

ELBE 1.3 GHz, 3-1/2-cell SRF Gun

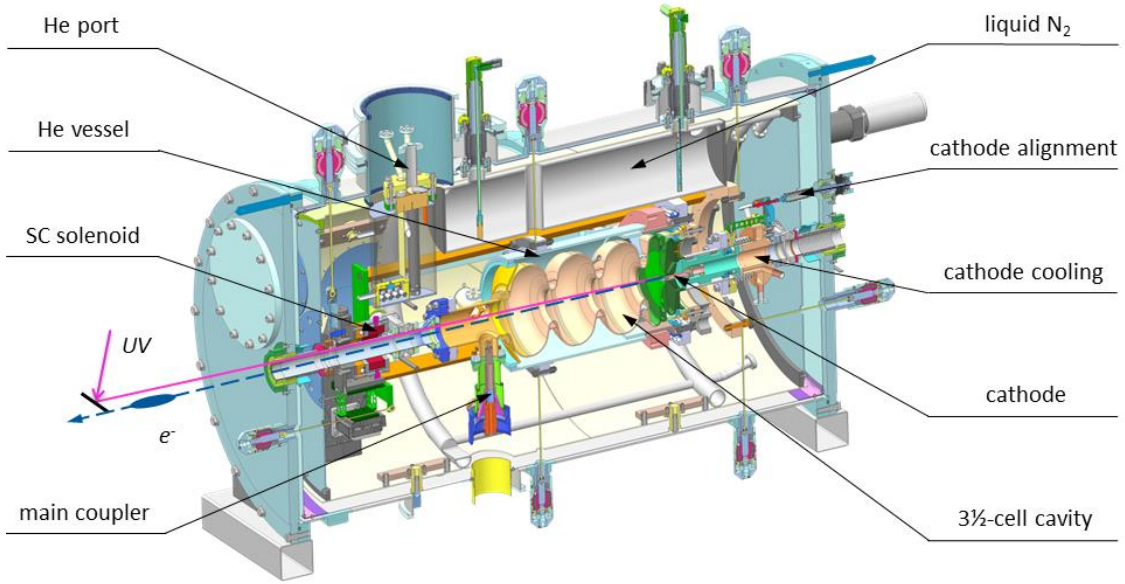

Parameter	SRF Gun II	SRF Gun III
Gradient	8 MV/m	12 MV/m
Peak field on axis	20.5 MV/m	30.7 MV/m
Kinetic energy	4 MeV	6 MeV
Bunch charge	300 pC	500 pC
Beam current	30 µA	50 µA,[1] 500 µA[2]
Pulse rep. rate	0.1-0.5 MHz,[1] 13MHz[2]	0.025-1 MHz,[1] 13 MHz[2]
Photocathode	Mg, Cs_2Te	Mg, Cs_2Te
Quantum efficiency	0.2-0.3%,[1] >1 %[2]	0.2%,[1] >1%[2]
Dark current	35 nA	<50 nA

[1] Mg cathode, [2] Cs2Te cathode

J. Teichert et al., “DESIGN UPGRADES OF THE NEXT SUPERCONDUCTING RF GUN FOR ELBE”,MOP100,SRF 2019.

The Peking University Hybrid Gun

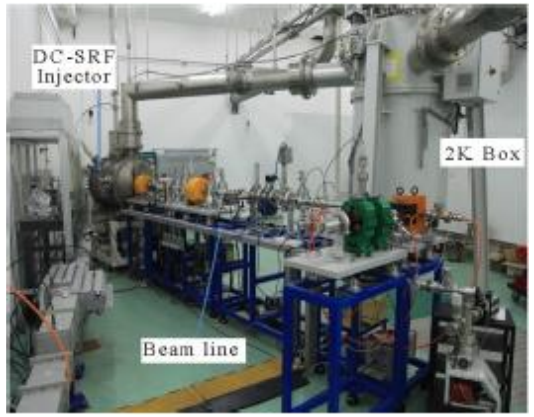

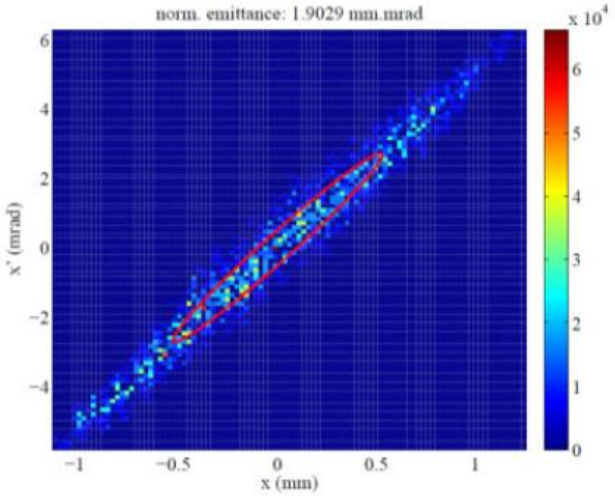

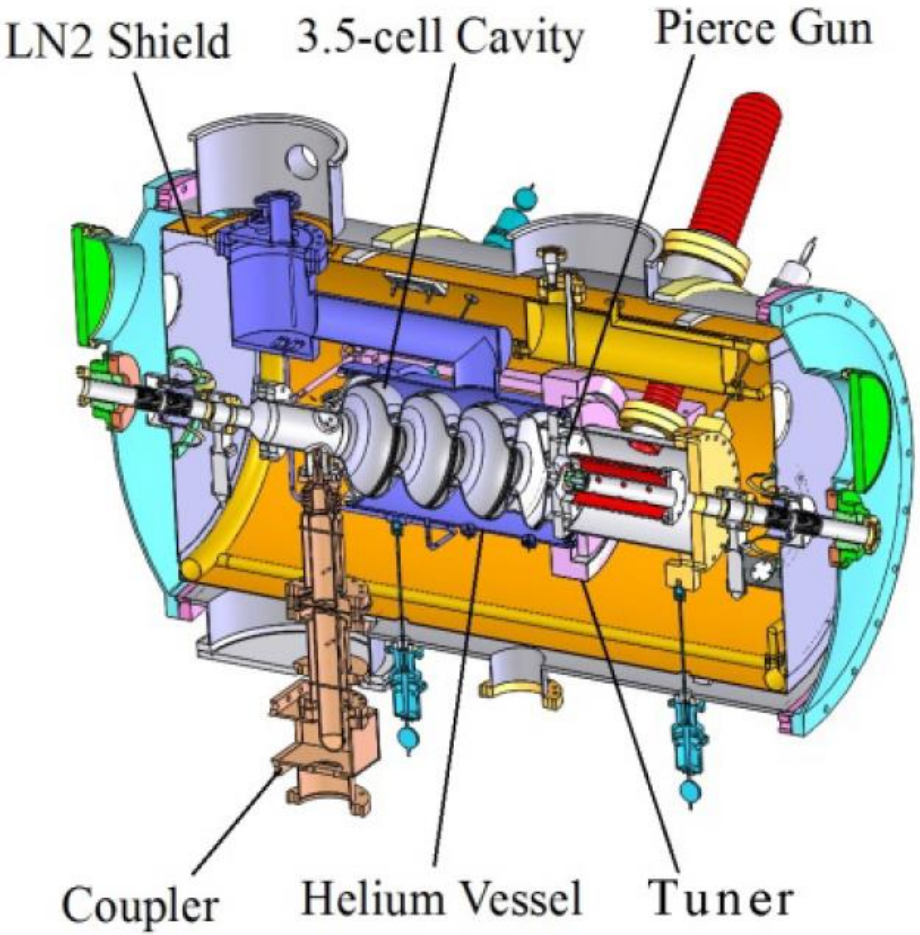

- CsTe photocathode outside cryogenic environment.
- Pierce gun with cathode voltage at -90 kV.
- 1.3 GHz, 3.5-cell SRF cavity providing 23.5 MV/m accelerating gradient to boost beam energy 3.4 MeV.
- Laser pulse repetition rate at 81.25 MHz
- RF pulse repetition rate at 10 Hz; macropulse beam current at 1 mA.
- Beam emittance of 1.9 mm-mrad has been measured.

J. Hao et al., WEPMN013 in IPAC 2015 proceedings (2015).

Transverse Space Charge Force

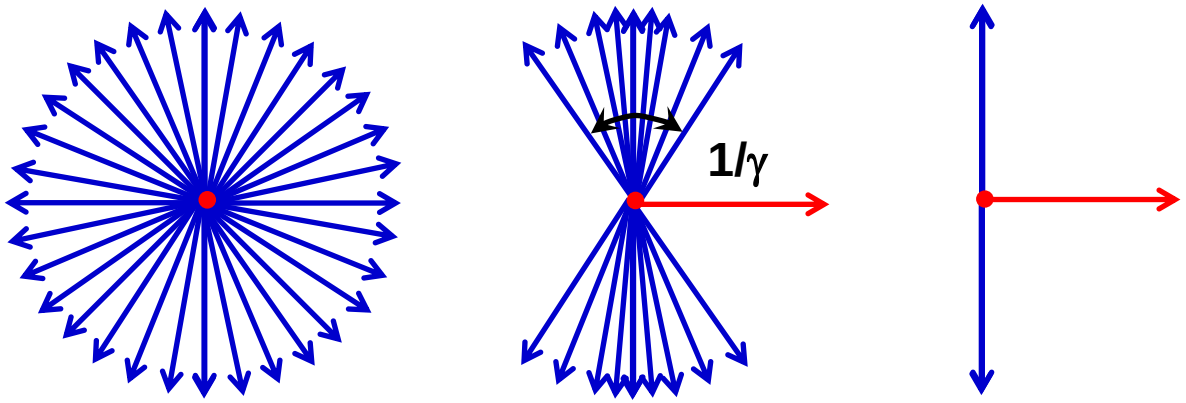

v = 0 v < c v = c

electric fields of a uniformly moving charged particle

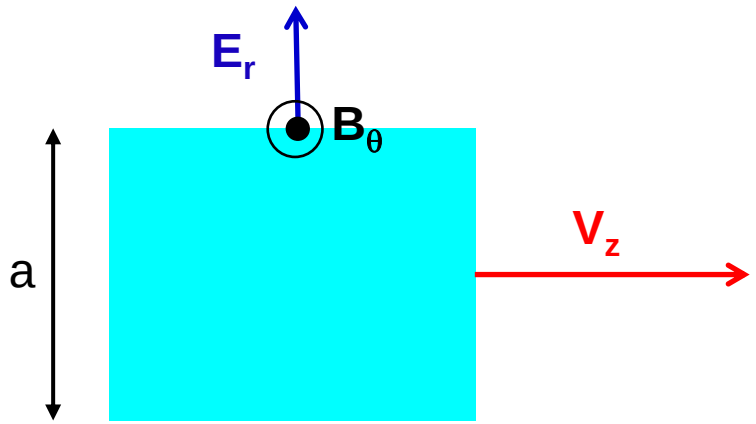

cylindrical electron bunch

Consider a cylindrical electron bunch with current I, uniform charge and current density ρ and J:

$$\rho = \frac{I}{\pi a^2 v_z} \qquad J = \frac{Ir}{\pi a^2}$$

Transverse space charge fields for *r < a:*

$$E_r = \frac{\rho r}{2\varepsilon_0} \qquad B_\theta = \frac{\mu_0 J r}{2} = \frac{v_z}{c^2} E_r$$

Lorentz force:

$$F_r = e(E_r - v_z B_\theta) = eE_r(1-\beta^2)$$

$$F_r = \frac{eE_r}{\gamma^2} \qquad \text{v} \rightarrow \text{c},\ F_r \rightarrow 0$$

Space Charge Force

a bunch of relativistic electrons can be viewed as a collection of independent slices

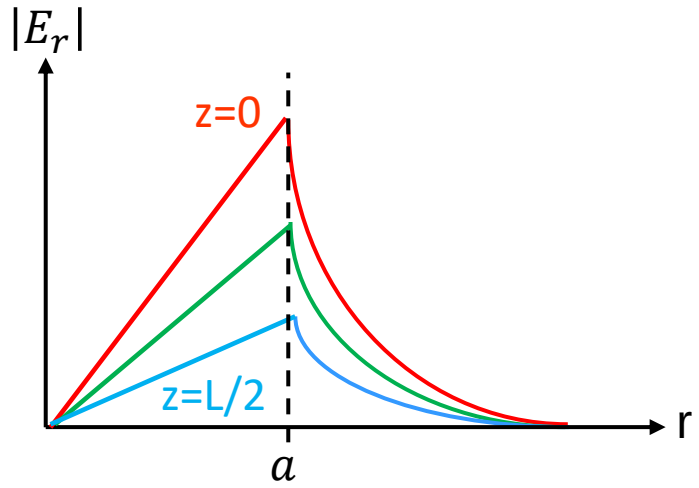

Transverse space charge force is highest at z=0

Projected emittance

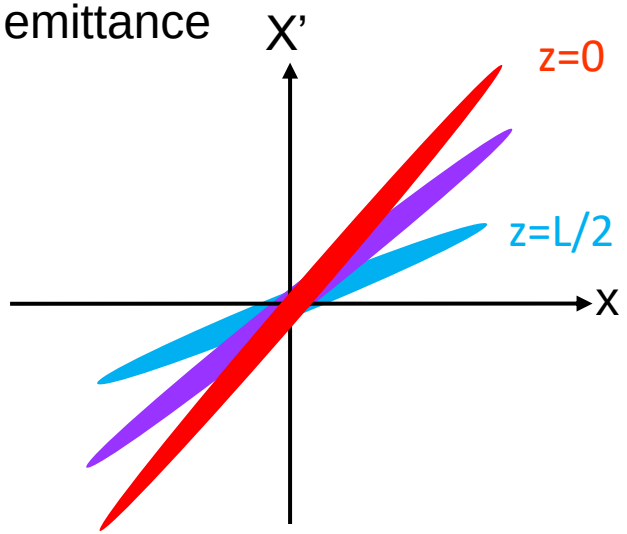

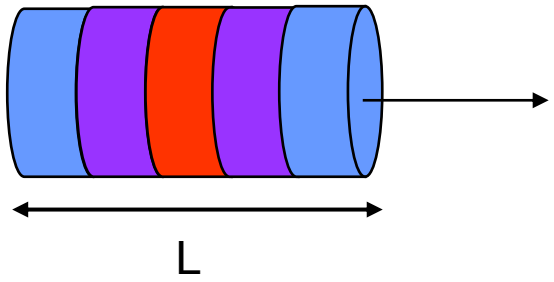

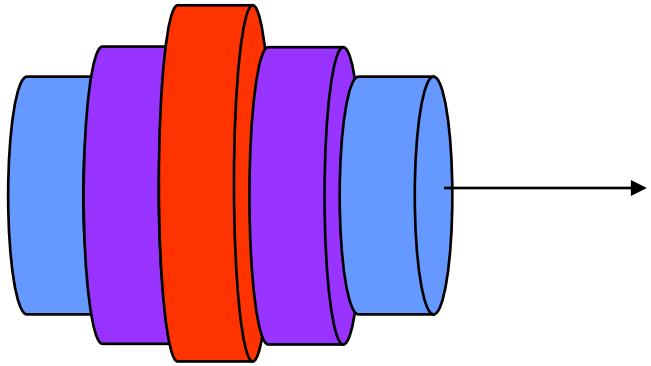

Different slices expand radially at different rate

Emittance Reduction Techniques

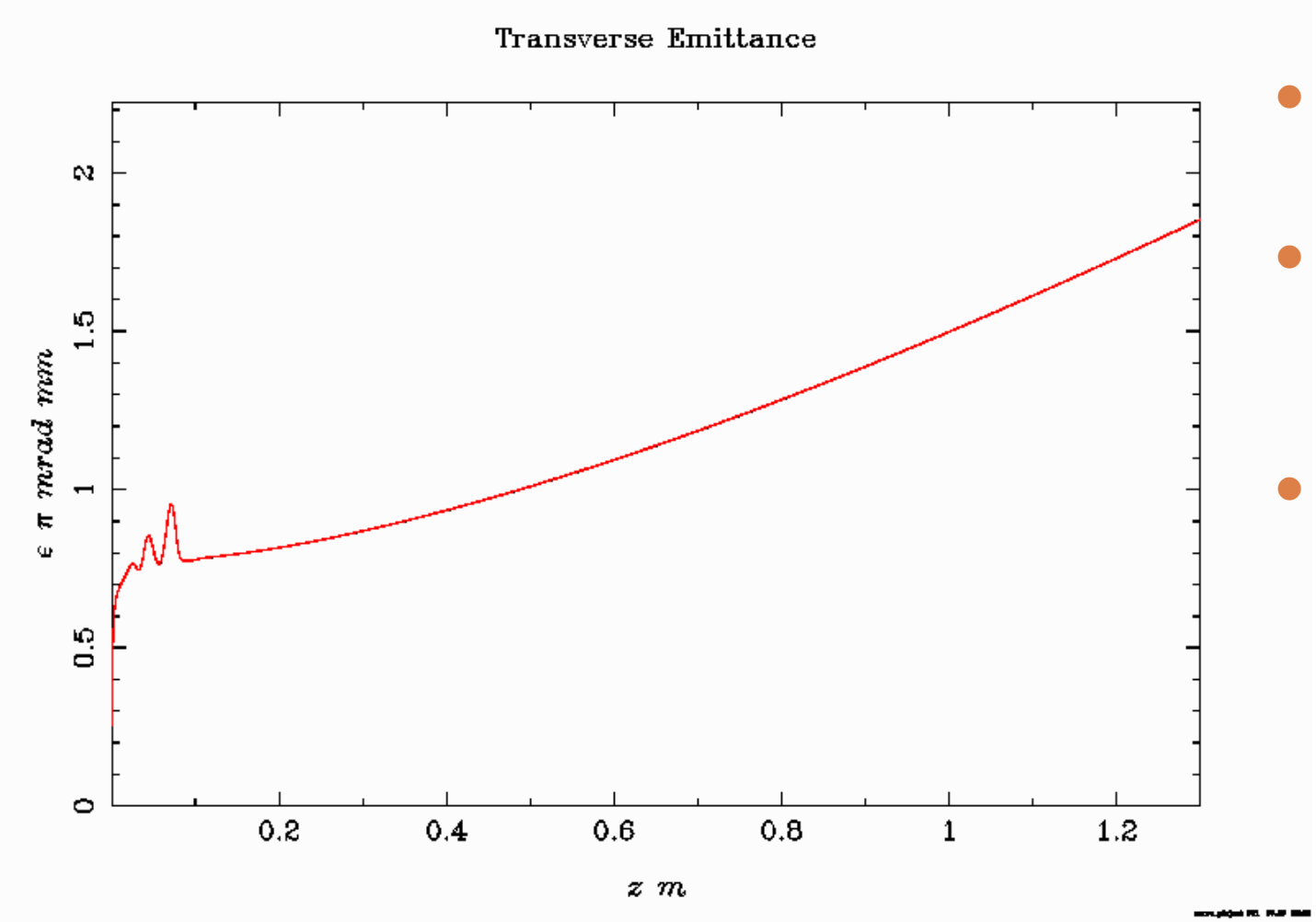

- Emittance grows continuously after leaving the gun cavity.
- Control of emittance is essential in high brightness electron beam design
- Reduction techniques of space charge:
  - emittance compensation solenoid
  - Shaping of electron distribution with laser

Emittance Compensation

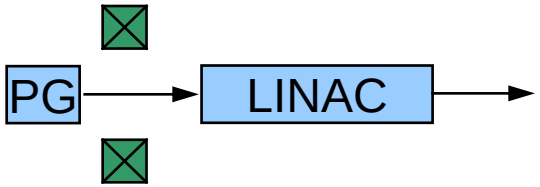

Evolution of normalized RMS emittance

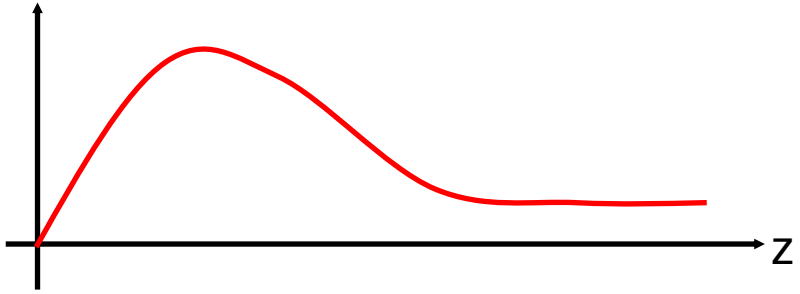

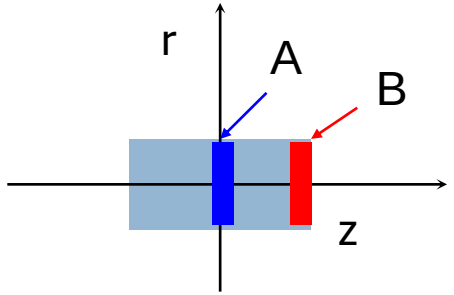

an electron bunch from the photo-cathode rf gun, particles near A experience different space charge force from particles near B

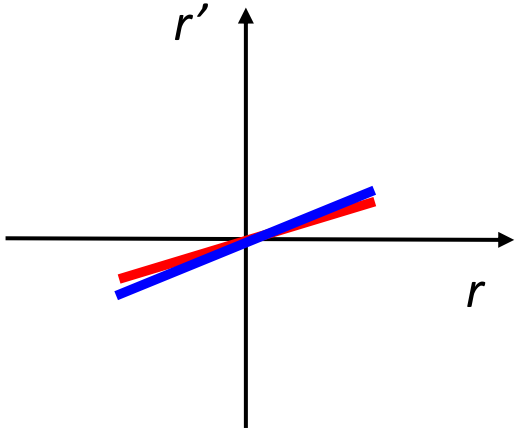

beam at gun exit

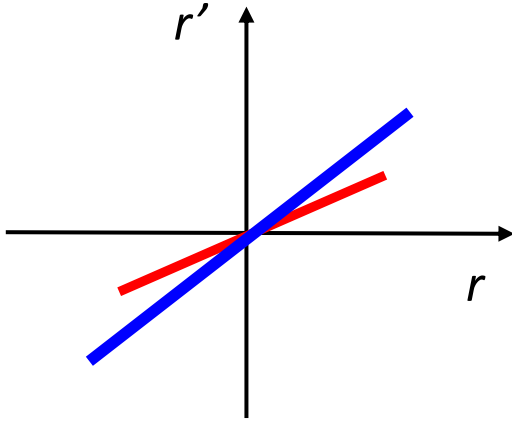

after a drift section

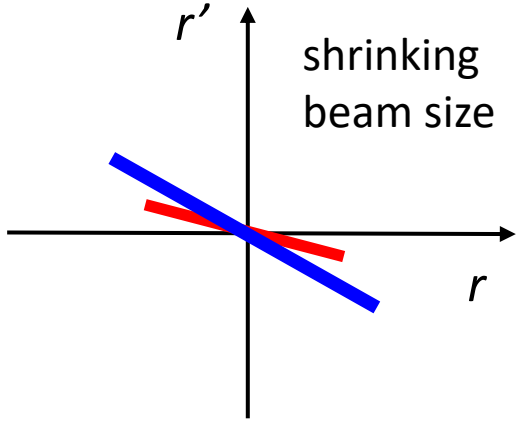

shrinking beam size

after focusing solenoid

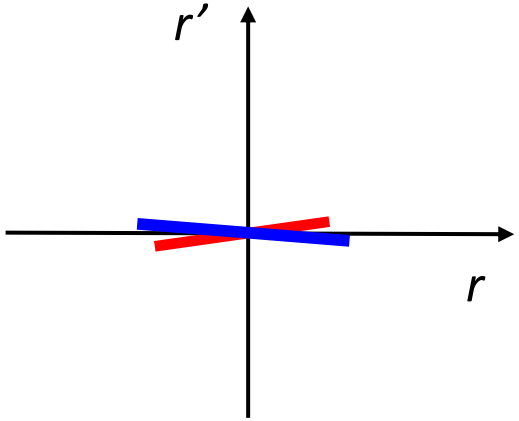

close to focal point of slice A

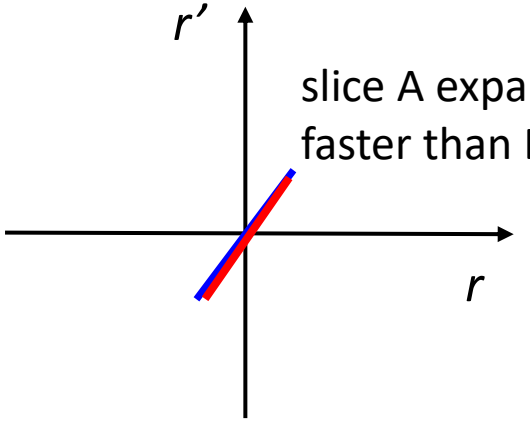

slice A expands faster than B

after focal point of slice A

Focusing realign slice emittance reducing projective emittance

Matching to Linac

- To keep the low emittance obtained, the emittance oscillations exactly in the point we want can be freeze by acceleration.
- An optimum injection condition, the invariant envelope matching condition into the Linac:

$$\sigma_{in} = \frac{2}{\gamma'}\sqrt{\frac{I_p}{2I_0\gamma}} \qquad \sigma'_{in} = -\frac{\gamma'}{2\gamma}\sigma_{in}$$

$$\sigma' = 0 \qquad \gamma' = \frac{eE}{mc^2}$$

$$\gamma' = \frac{2}{\sigma}\sqrt{\frac{I_p}{2I_0\gamma}}$$

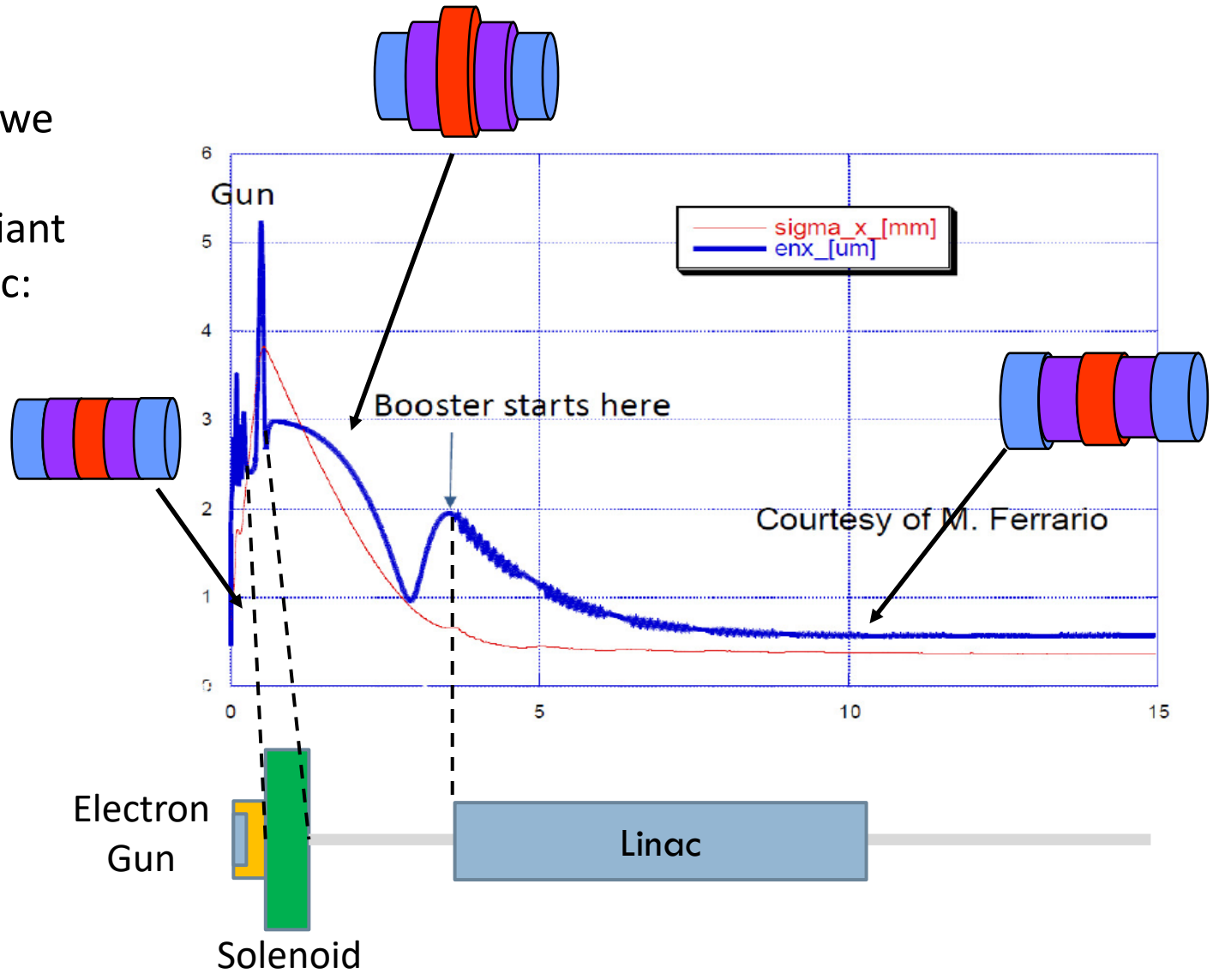

Emittance Control by Laser Pulse Shaping

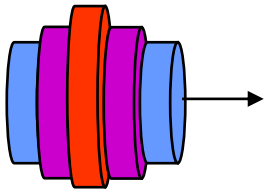

Different slices in a non-uniform bunch (e.g. Gaussian) experience different space charge force, emittance compensation by solenoid will be difficult.

- Uniform transverse profile
- Flattop temporal profile

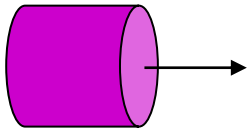

A uniform cylindrical electron beam can reduce emittance (an ellipsoid will be ideal)

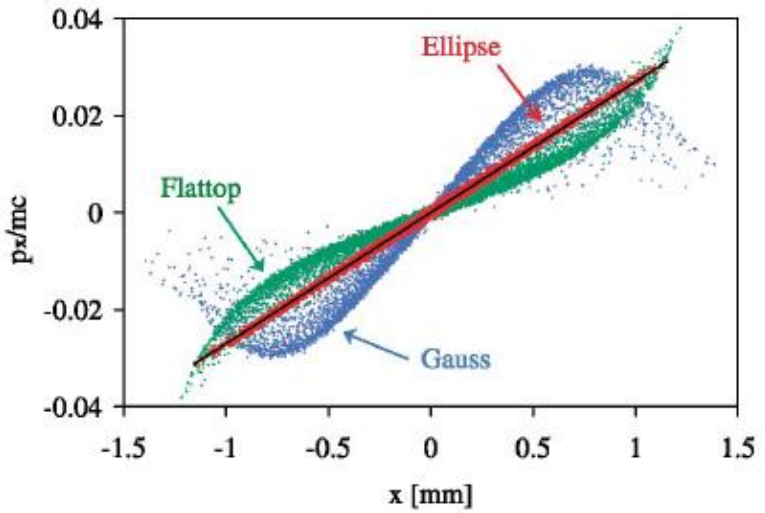

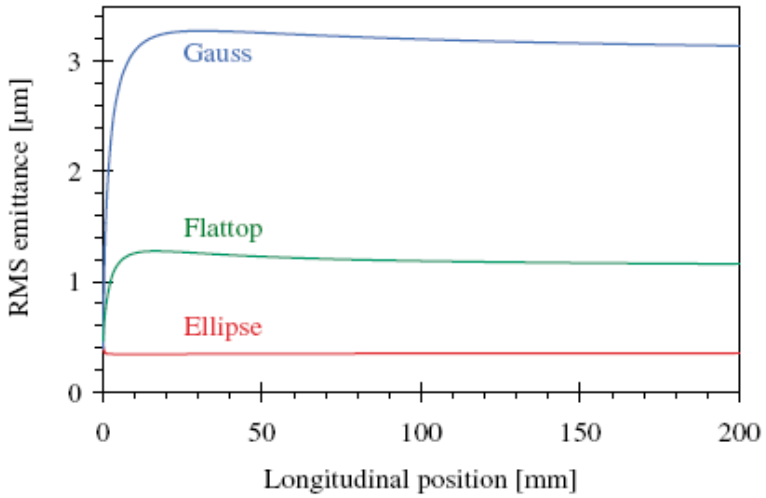

(O.J. Luiten et al., PRL 094802, 2004)

Outline

- Beam emittance and brightness
- Electron Source
- Electron guns
- **Bunch compressor**
- Beam diagnostics

Bunch Compression with Magnets

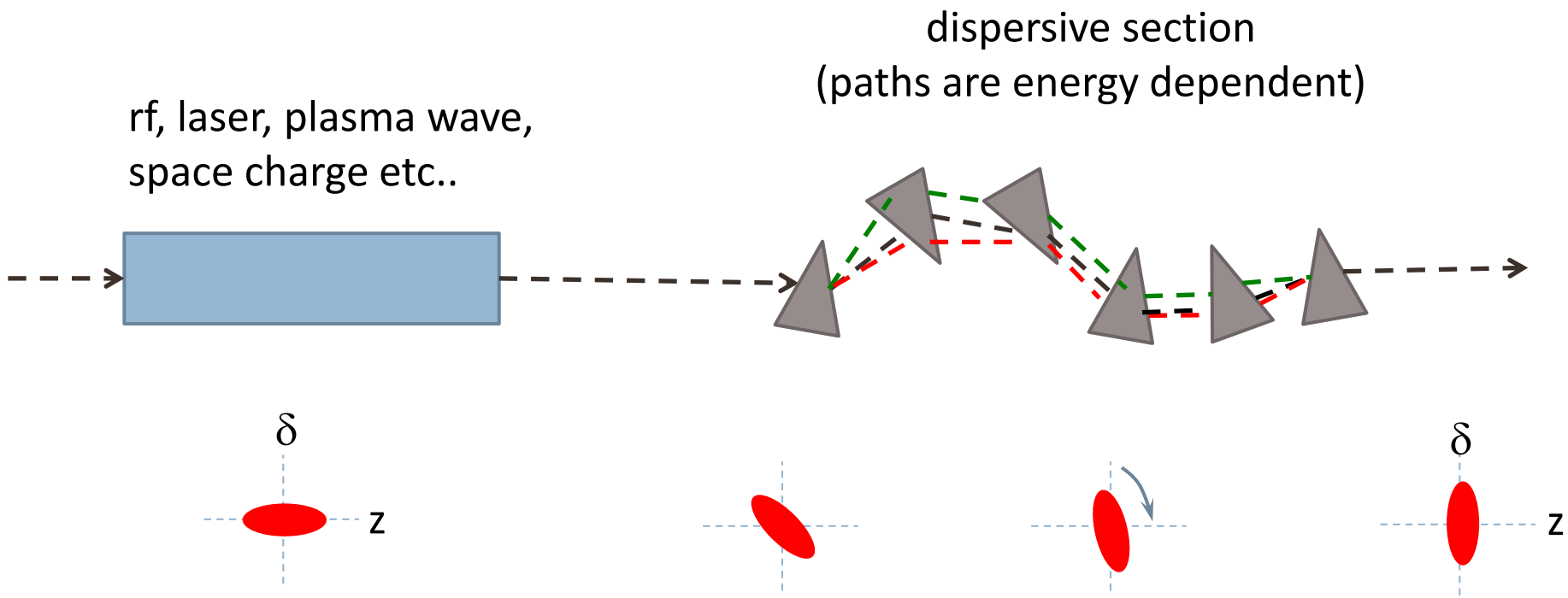

isochronous !!

it can be part of a drive linac system for FEL or a ring lattice for low momentum compaction operation.

Beam Transport Notations

the particle motion in a 6-D phase space can be described by transfer matrices

$$\left[\vec{X}\right]_2 = \mathrm{M}\left[\vec{X}\right]_1, \qquad \vec{X} = (x, x', y, y', z, \delta), \quad \delta = \Delta E / E = \Delta\gamma / \gamma$$

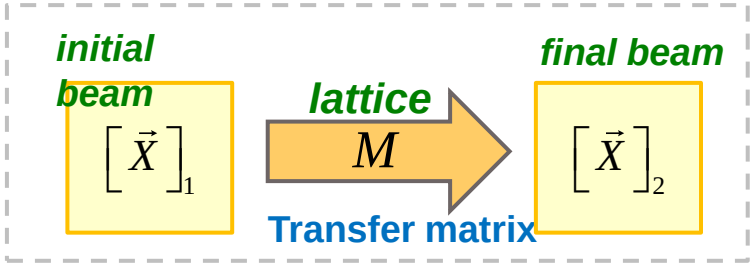

(Example of beam transport line)

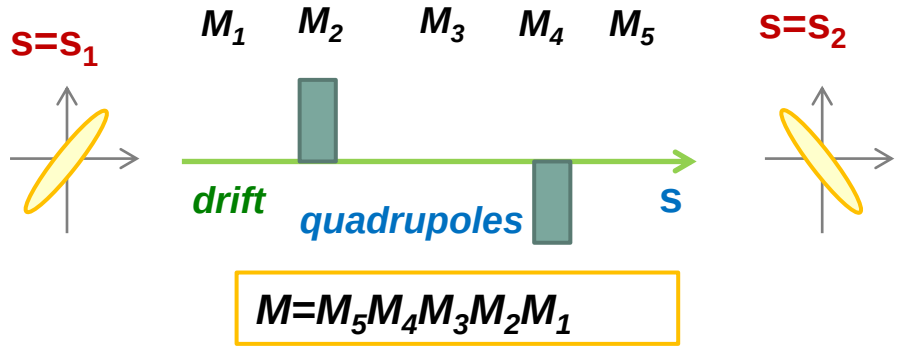

$M=M_5M_4M_3M_2M_1$

$$\begin{bmatrix} x(s_2) \\ x'(s_2) \\ y(s_2) \\ y'(s_2) \\ z(s_2) \\ \delta(s_2) \end{bmatrix} = \begin{bmatrix} R_{11} & R_{12} & R_{13} & R_{14} & R_{15} & R_{16} \\ R_{21} & R_{22} & R_{23} & R_{24} & R_{25} & R_{26} \\ R_{31} & R_{32} & R_{33} & R_{34} & R_{35} & R_{36} \\ R_{41} & R_{42} & R_{43} & R_{44} & R_{45} & R_{46} \\ R_{51} & R_{52} & R_{53} & R_{54} & R_{55} & R_{56} \\ R_{61} & R_{62} & R_{63} & R_{64} & R_{65} & R_{66} \end{bmatrix} \begin{bmatrix} x(s_1) \\ x'(s_1) \\ y(s_1) \\ y'(s_1) \\ z(s_1) \\ \delta(s_1) \end{bmatrix},$$

where

$R_{11}(x|x_0)$,

$R_{12}(x|x'_0),\ldots$

$R_{26}(x'|\delta_0)$,

$R_{56}(z|\delta_0), T_{566}(z|\delta_0^2), U_{5666}(z|\delta_0^3),\ldots$

$$z(s_2) = z(s_1) + R_{56}\delta + T_{566}\delta^2 + U_{5666}\delta^3 + \cdots$$

Energy Chirper after Linac

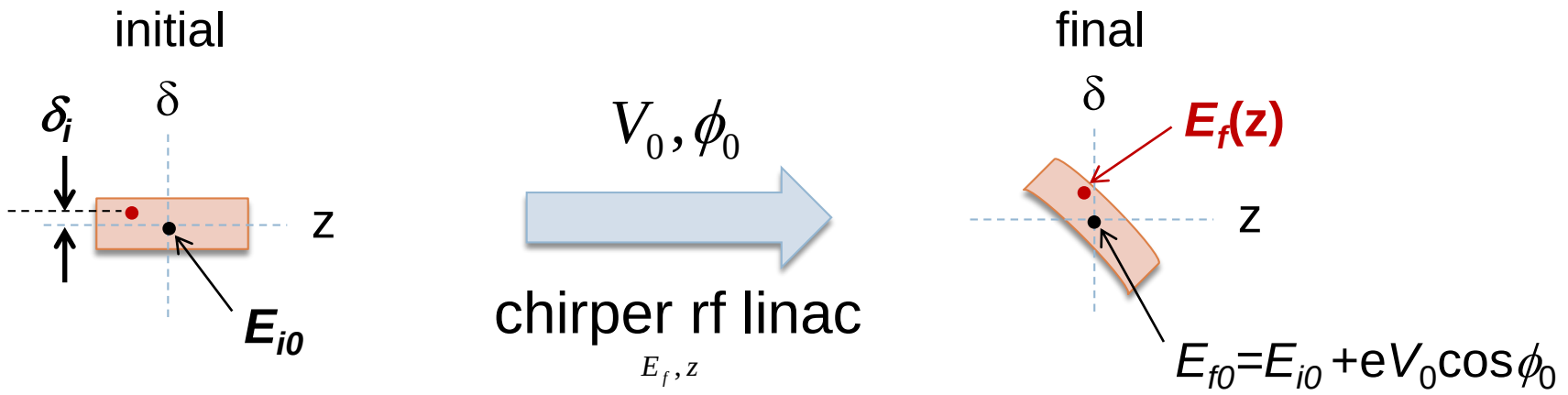

$$E_f(z) = E_{i0}(1+\delta_i) + eV_0\cos(\phi_0 - kz)$$

$$= E_{f0} + E_{i0}\delta_i + keV_0\sin(\phi_0)z - \frac{k^2eV_0}{2}\cos(\phi_0)z^2 - \frac{k^3eV_0}{6}\sin(\phi_0)z^3 + \cdots$$

$$E_{f0} = E_{i0} + eV\cos\phi_0$$

Energy Chirper after Linac

$$\delta(z)=\frac{E_f(z)-E_{f0}}{E_{f0}}=a\delta_i+h_1z+h_2z^2+h_3z^3+\cdots$$

$-\pi/2<\phi_0<\pi/2$

$$\begin{cases} a=E_{i0}/E_{f0} & \text{‘damping factor’} \\ h_1=\dfrac{keV_0}{E_{f0}}\sin\phi_0 & \text{‘1st order energy chirp’} \\ h_2=-\dfrac{k^2eV_0}{2E_{f0}}\cos\phi_0 & \text{‘2nd order energy chirp’ (always -ve for accelerating phases)} \\ h_3=-\dfrac{k^3eV_0}{6E_{f0}}\sin\phi_0 & \text{‘3rd order energy chirp’} \end{cases}$$

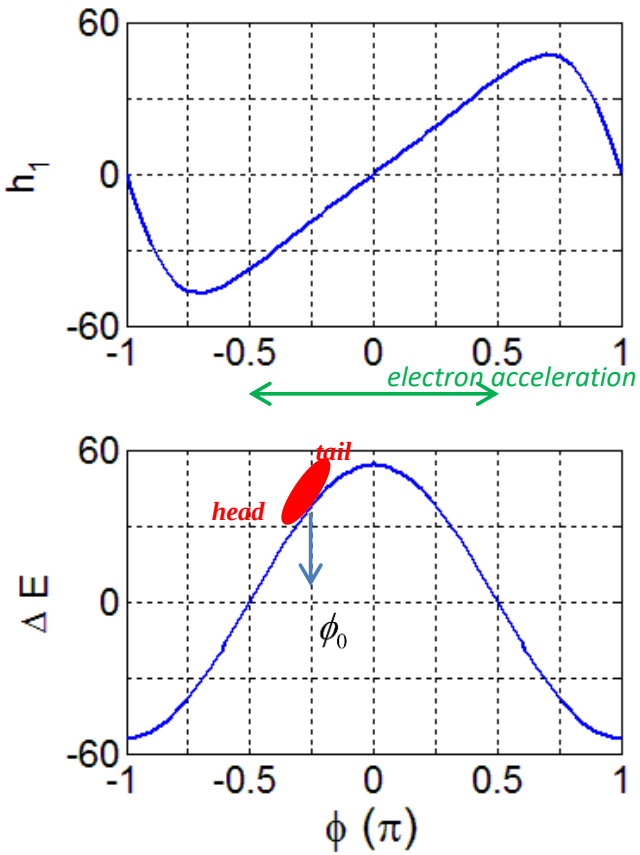

Electron Position after the Dispersive Section

$$z_f = z_i + R_{56}\delta + T_{566}\delta^2 + U_{5666}\delta^3 + \cdots$$

$$z_f = z_i + R_{56}\left(a\delta_1 + h_1 z_i + h_2 z_i^2 + h_3 z_i^3\right) + T_{566}\left(h_1 z_i + h_2 z_i^2 + h_3 z_i^3\right)^2 + U_{5666}\left(h_1 z_i + h_2 z_i^2 + h_3 z_i^3\right)^3 + \cdots$$

$$z_f = aR_{56}\delta_i + \left(1 + h_1 R_{56}\right)z_i + \left(h_2 R_{56} + h_1^2 T_{566}\right)z_i^2 + \left(h_3 R_{56} + 2h_1 h_2 T_{566} + h_1^3 U_{5666}\right)z_i^3 + \cdots$$

we considered here more nonlinear terms, R_{56}, T_{566}, U_{5666} are the first, second and third order longitudinal dispersion respectively.

the initial uncorrelated energy spread for higher order terms has been neglected.

expression for the longitudinal position of an electron after a compressor system which includes an rf chirper linac section.

RMS Bunch Length after Compression

$$\sigma_z = \sqrt{\langle z^2 \rangle} = \sqrt{\int z_f^2 f(z_f) dz_f}\,.$$

the RMS electron bunch length is the expectation value of longitudinal position for a distribution of electrons $f(z_f)$

$$z_f^2 = (aR_{56}\delta_i)^2 + \left[(1+h_1R_{56})^2\right] z_i^2$$

$$+ \left[(h_2R_{56} + h_1^2T_{566})^2 + 2(1+h_1R_{56})(h_3R_{56} + 2h_1h_2T_{566} + h_1^3U_{5666})\right] z_i^4 + \cdots.$$

here we assumed an Gaussian distribution of electrons !!

if we ignore initial energy spread and other higher order terms, we can define a *linear compression factor C* ,

$$C = \frac{1}{1+h_1R_{56}} = \frac{\sigma_{zi}}{\sigma_z}.$$

for high compression ratio, first order energy chirp h_1 and first order longitudinal dispersion R_{56} should have opposite signs such that $1+h_1R_{56} \approx 0$.

R_{56} and T_{566} of a 4-dipole Chicane

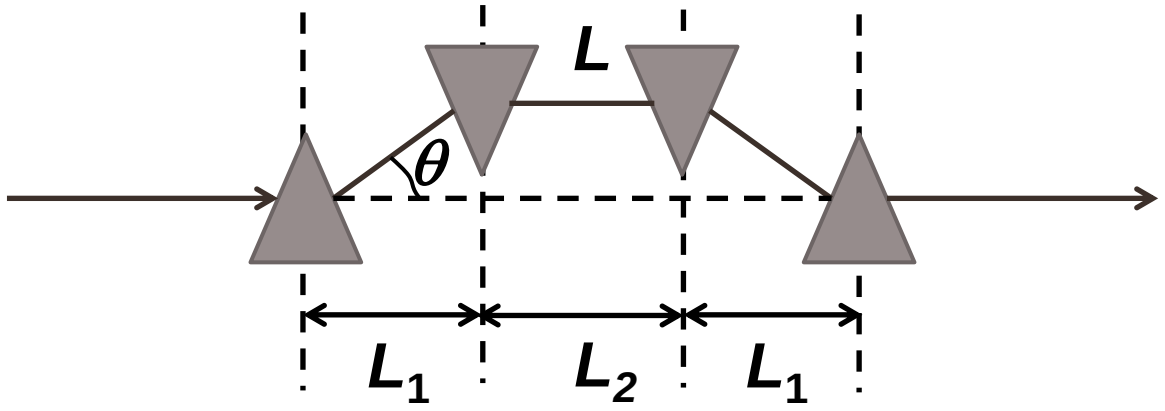

$$L = \frac{2L_1}{\cos\theta} + L_2$$

$$\theta = \frac{\theta_0}{1+\delta}$$

$$\delta_2 = \delta_1$$

$$z_2 = z_1 + 2L_1\left(\frac{1}{\cos\theta_0} - \frac{1}{\cos\theta}\right)$$

a nonlinear function of δ, can be expanded in terms of δ as Taylor series about θ_0 .

$$z_2 \approx z_1 + \underbrace{2L_1\theta_0^2\delta}_{R_{56}} \underbrace{- 3L_1\theta_0^2\delta^2}_{T_{566}} + \cdots$$

for $\theta << 1$ ⇒

$$\frac{T_{566}}{R_{56}} \approx -\frac{3}{2}$$

R_{56} is always positive and T_{566} is always nagtive

Bunch Compressor with 4 Dipoles

dispersive section
(paths are energy dependent)

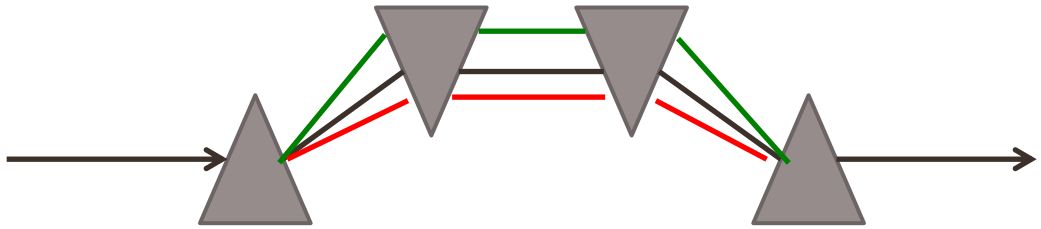

$\Delta z = R_{56}\delta < 0$ for –ve δ

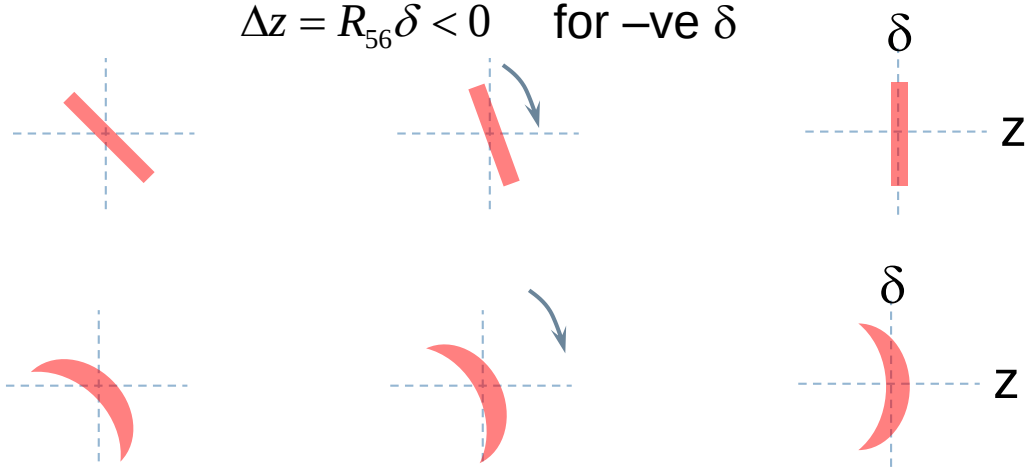

Since for max. linear compression ratio

$$R_{56} = -\frac{1}{h_1} > 0$$

this forced us to operate rf phase in the range $\boxed{-\pi/2 < \phi_0 < 0}$ such that $h_1 < 0$.

If we want to cancel the effect of second order energy chirps also, we also require

$$T_{566} = -\frac{h_2 R_{56}}{h_1^2} > 0$$

since R_{56} is always *+ve* for a 4-rectangular dipole chicane and h_2 is always *-ve* for all accelerating phases.

However, T_{566} is always *–ve* for this type of chicane. Therefore, it is not possible to compensate the effect of *2*nd order chirp in this situation.

Harmonic Compensation of 2nd Order Energy Chirp

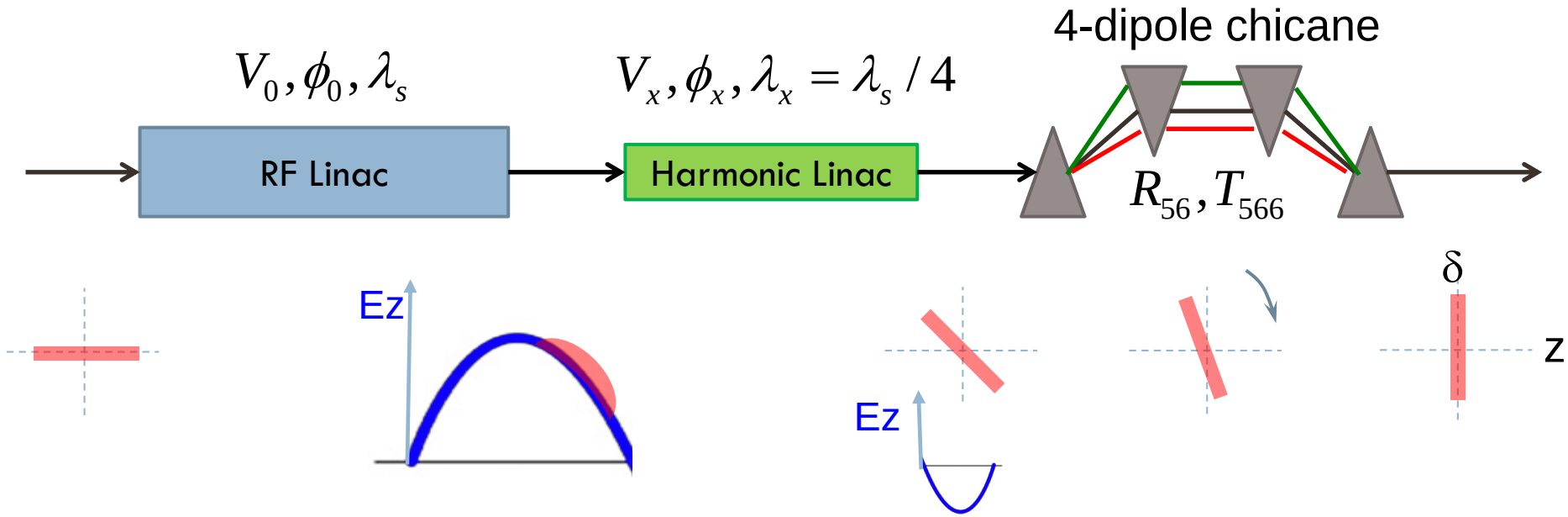

$$E_f(z) = E_{i0}(1+\delta_i) + eV_0\cos(\phi_0 - k_s z) + eV_x\cos(\phi_x - k_x z)$$

$$= E_{f0} + E_{i0}\delta_i + k_s eV_0 \sin(\phi_0) z - \frac{k_s^2 eV_0}{2}\cos(\phi_0) z^2 -$$

$$+ \frac{k_x^2 eV_x}{2} z^2 + \cdots$$

expand cos(ϕ_x-$k_x z$) about $\phi_x = \pi$

Harmonic Compensation of 2nd Order Energy Chirp

$$\delta_f = \frac{E_{i0}\delta_i}{E_{f0}} + \frac{k_s eV_0}{E_{f0}}\sin(\phi_0)\cdot z + \left[\frac{-k_s^2 eV_0\cos(\phi_0) + eV_x k_x^2}{2E_{f0}}\right]\cdot z^2$$

$$\delta_f = a\delta_i + h_1 z + h_2 z^2 + \cdots$$

$$\begin{cases} a = E_{i0}/E_{f0} \\ h_1 = \dfrac{k_s eV_0}{E_{f0}}\sin\varphi_0 \\ h_2 = \dfrac{-k_s^2 eV_0\cos(\varphi_0) + eV_x k_x^2}{2E_{f0}} \end{cases}$$

Harmonic Compensation of 2nd Order Energy Chirp

$$z_f = aR_{56}\delta_i + \underbrace{(1 + h_1 R_{56})}z_i + \underbrace{(h_2 R_{56} + h_1^2 T_{566})}z_i^2$$

we require that these two coefficients vanish for optimum compression

that is $$h_2 = -\frac{T_{566}}{R_{56}} h_1^2$$

choose rf phase of x-band cavity such that h2 is being +ve

$$\frac{-eV_0 k_s^2 \cos\phi_0 + eV_x k_x^2}{2E_{f0}} = -\frac{T_{566}}{R_{56}}\left(\frac{eV_0 k_s \sin\phi_0}{E_{f0}}\right)^2$$

condition for harmonic compensation of 2nd order energy chirp for 4-dipole chicane

$$T_{566}/R_{56} \approx -1.5$$

- Beam emittance and brightness
- Electron Source
- Electron guns
- Bunch compressor
- **Beam diagnostics**

Bunch Charge Measurement

Intercepting diagnostic: ***the Faraday cup***

- The FC is a beam stopper that can be inserted when needed in the beam line.
- An isolated metal cup stops the beam. The electron current is *directly* read by a readout electronics connected to the cup.

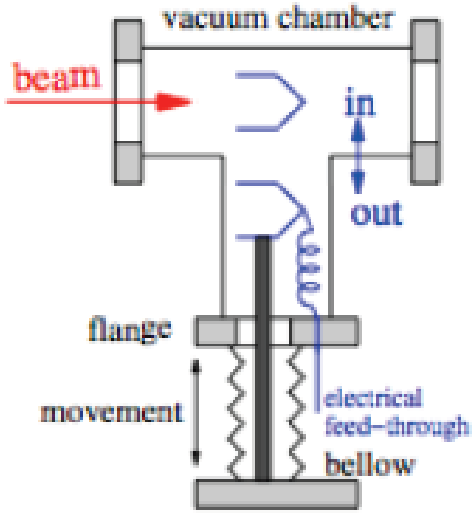

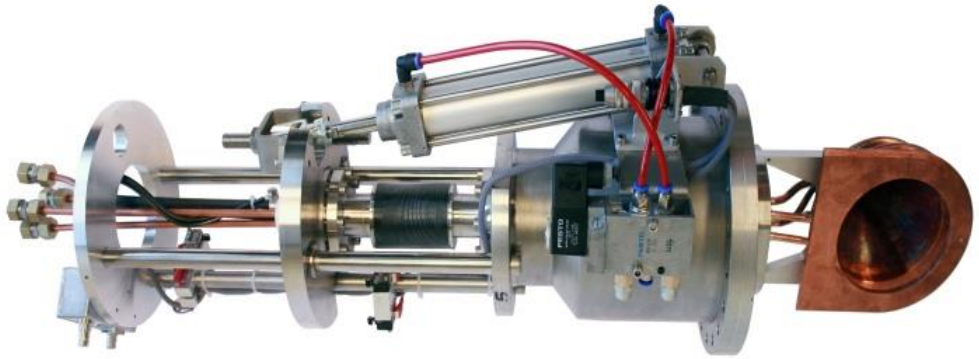

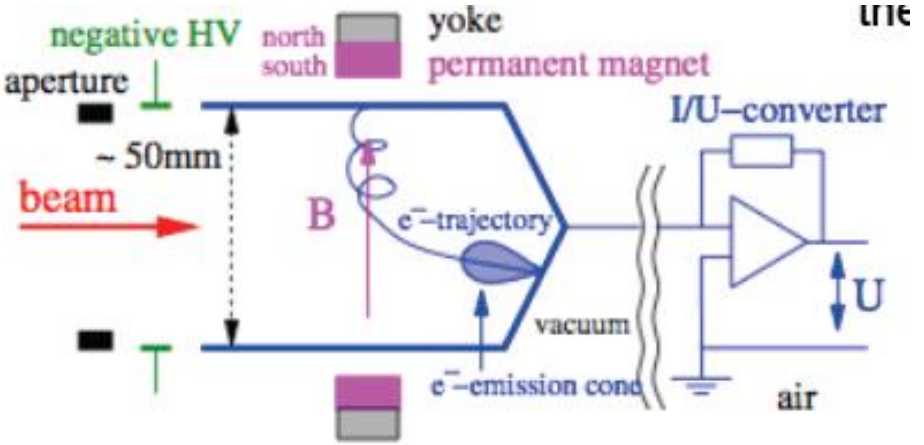

Bunch Charge Measurement

Non-Intercepting diagnostic: the ***beam current monitor***

- Beam used as primary winding of a transformer:

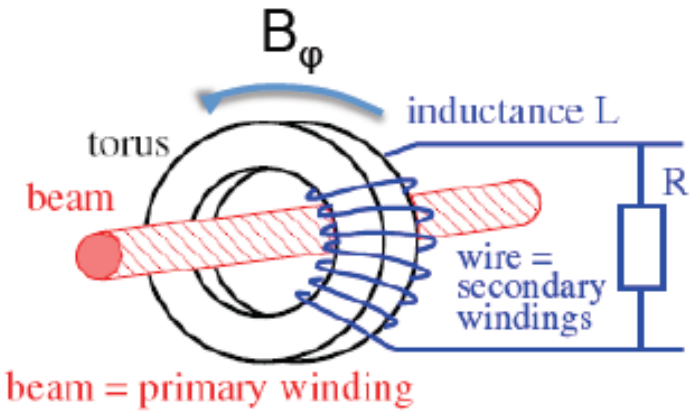

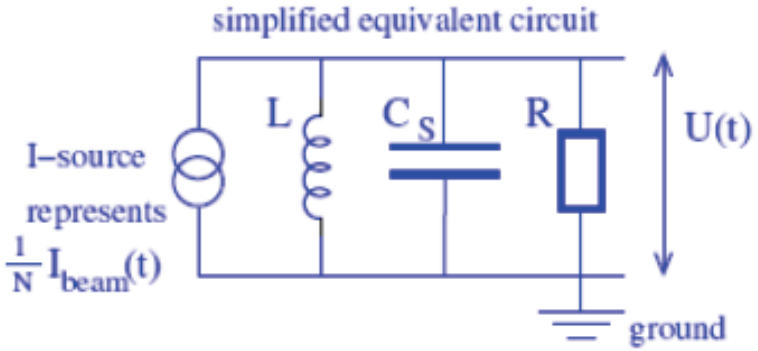

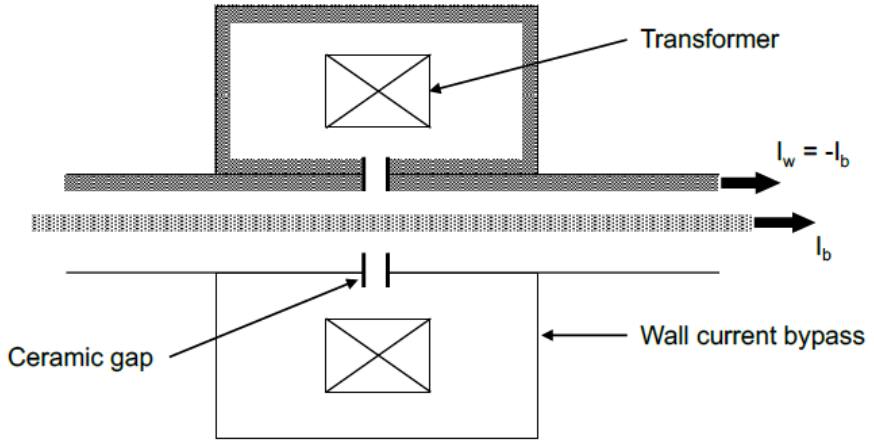

Beam Profile Measurement

- Destructive Measurement
- Measure current density as function of transverse coordinates
- Must verify screen and detector not saturated
- Common Screen Materials
  - Phosphor
  - YAG
  - OTR
  - Wire scaner

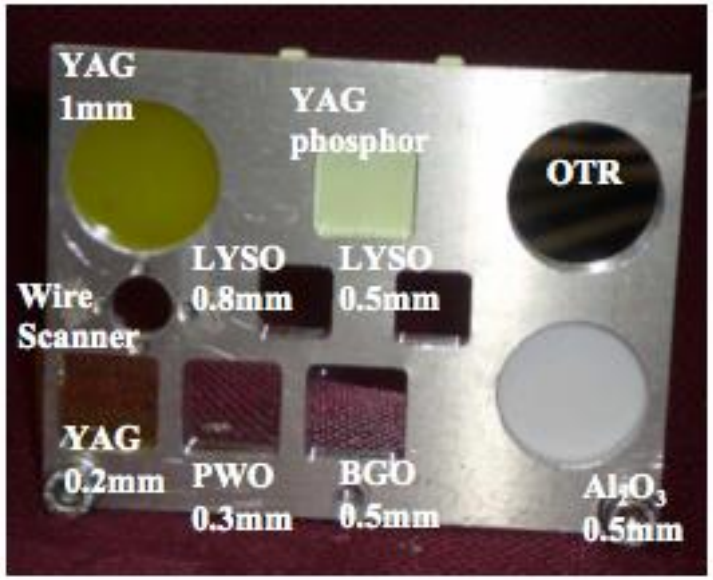

Screen	Resolution	Dynamic Range	Time Response
Phosphor	≈ 50 μm	small	ms
YAG	≈ 20 μm	medium	< ms
OTR	≈ 10 μm	large	fs
Wire	≈ 10 μm	large	ns

Energy Measurement

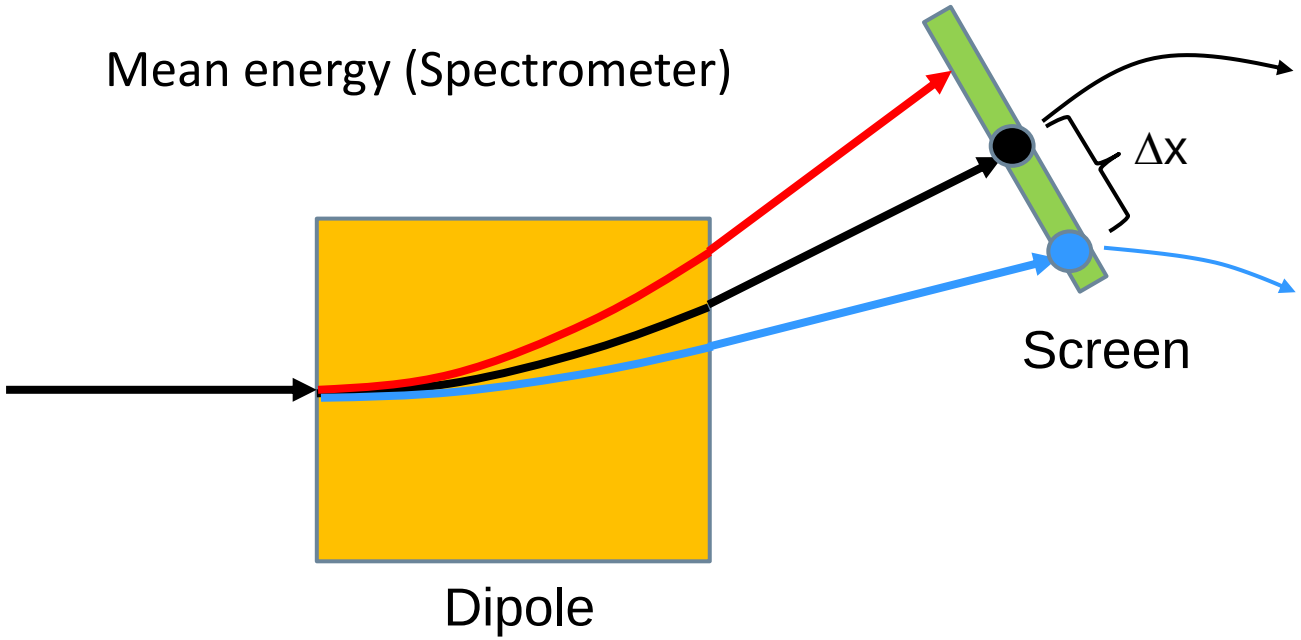

"on-energy" particle centers the screen

$$\langle p_z \rangle \left[\frac{GeV}{C}\right] = 0.3 B_{y0}[T] R[m]$$

"off-energy" particle centers the screen

$$p_z = \langle p_z \rangle \left(1 + \frac{\Delta x}{\eta_x}\right)$$

1. geometry of the ref. trajectory (q, R) is fixed by the mechanical assembly,
2. B_y is chosen to center the beam onto the detector (screen or BPM),
3. calculate $<p_z>$.

Emittance Measurement

- Quadruple scan for high energy beam when linear beam optics is valid, i.e. when space charge forces are small and energy spread is not too large

- Slit method for low energy beam when space charge forces are small, and beam can be stopped by the slit mask

	High Energy	High Space Charge Force	Large Energy Spread
3 Screen	+	-	+
Quadruple Scan	+	-	-
Slit	-	+	+

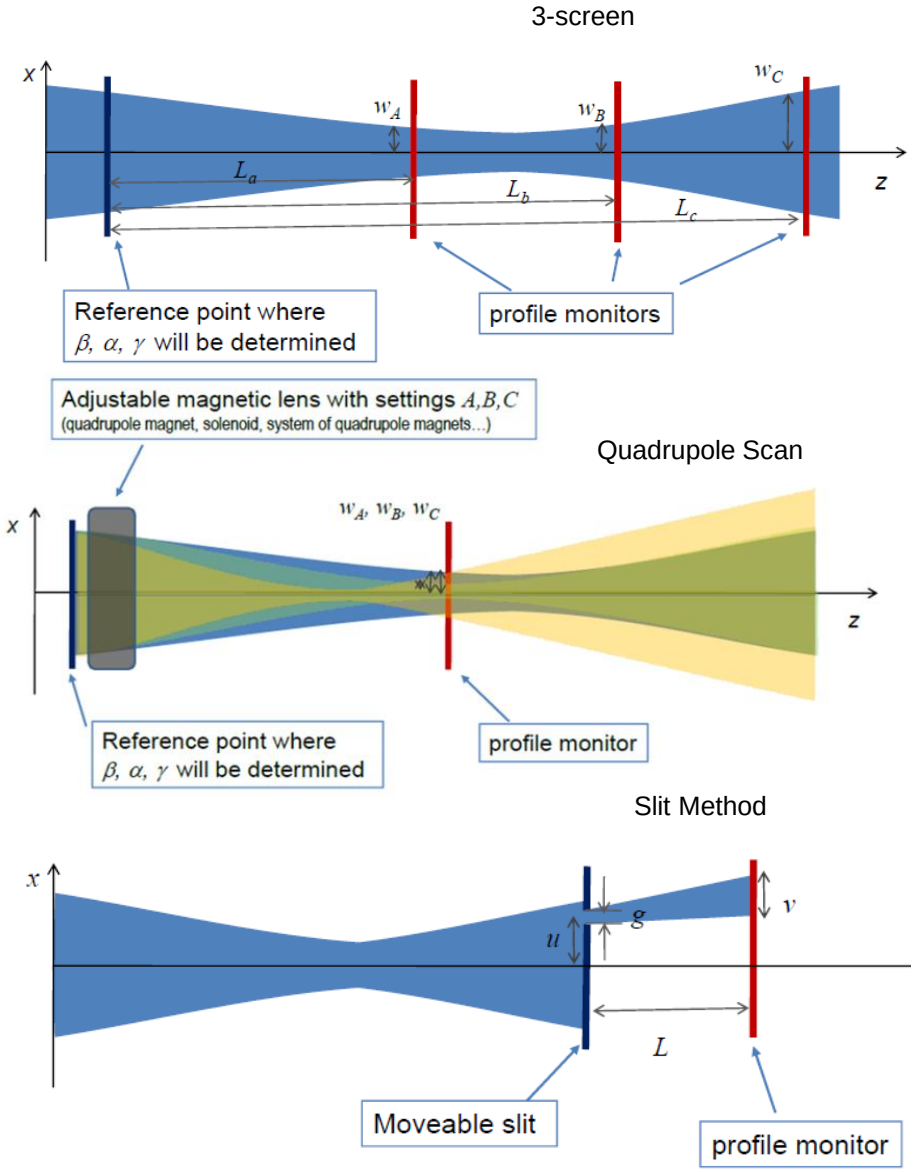

Emittance Measurement : Multi-slit or Pepper Pot

- To measure emittance requires emittance dominated beam
- Space charge dominated beam must be converted to emittance dominated
- N measurements made simultaneously
- Measure angle and spread downstream of slit on a screen as a function of slit position

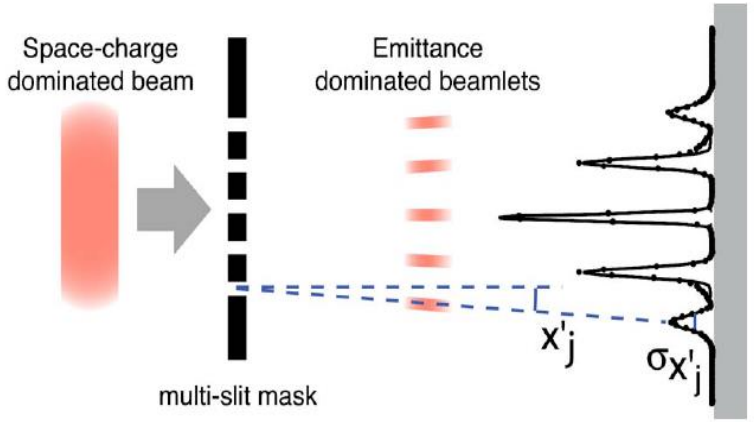

$$\epsilon_x{}^2 = < x^2 >< x'^2 > - < xx' >^2$$

$$\approx \frac{1}{N^2}\left\{\left[\sum_{j=1}^{p} n_j\left(x_{sj}-\bar{x}\right)^2\right]\left[\sum_{j=1}^{p}\left[n_j{\sigma_{x_j'}}^2 + n_j\left(\overline{x_j'}-\bar{x}\right)^2\right]\right] - \left[\sum_{j=1}^{p} n_j x_{sj}\overline{x_j'} - N\bar{x}\overline{x'}\right]^2\right\}$$

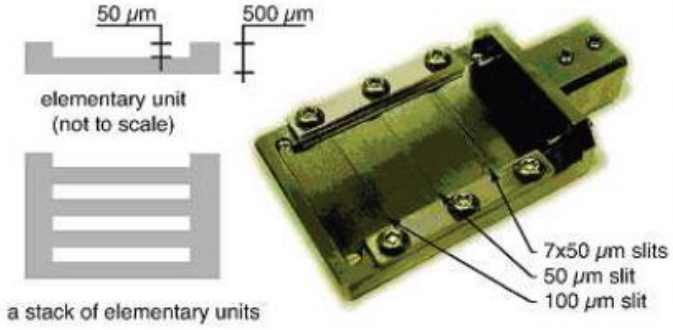

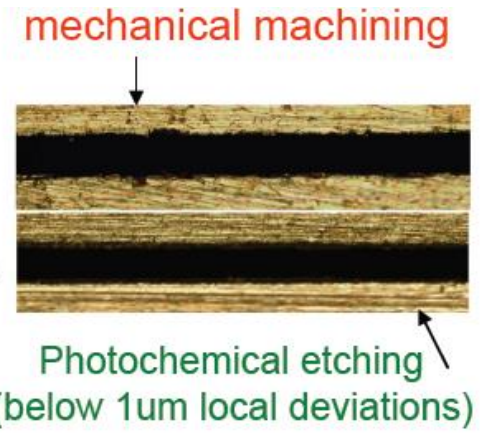

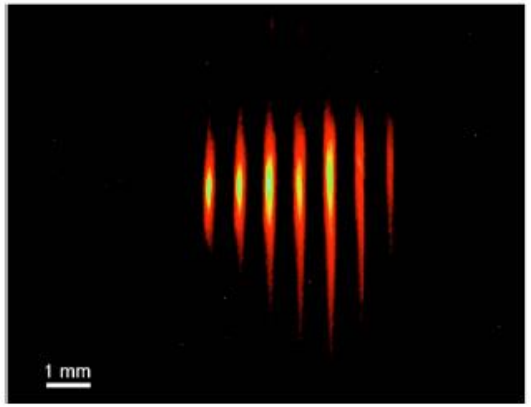

Emittance Measurement : Quadrupole Scan

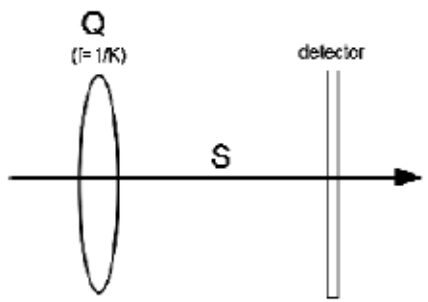

$$Q \cong \begin{pmatrix} 1 & 0 \\ K & 1 \end{pmatrix} \quad S = \begin{pmatrix} S_{11} & S_{12} \\ S_{21} & S_{22} \end{pmatrix}$$

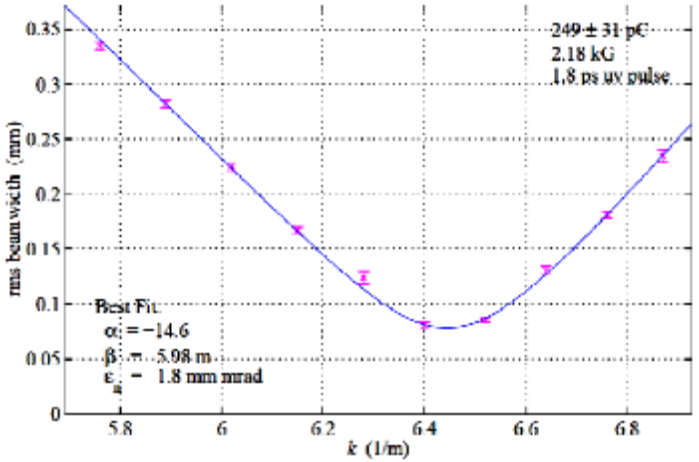

1. The transport matrix from the quadrupole (thin lens approximation) to the detector (screen) is assumed to be known:

$$T = QS = \begin{pmatrix} S_{11} + KS_{12} & S_{12} \\ S_{21} + KS_{22} & S_{22} \end{pmatrix}$$

2. The beam matrix transforms according to:

$$\Sigma_f = T\Sigma_0 T^t$$

3. The beam matrix element <x2> is quadratic in the quadrupole integrated strength K = kl:

$$\Sigma_{11}(= \langle x^2 \rangle) = (S_{11}{}^2\Sigma_{11_0} + 2S_{11}S_{12}\Sigma_{12_0} + S_{12}{}^2\Sigma_{22_0}) + (2S_{11}S_{12}\Sigma_{11_0} + 2S_{12}{}^2\Sigma_{12_0})K + S_{12}{}^2\Sigma_{11_0}K^2$$

4. Vary the quad strength k and measure σ_x at the screen. Then fit with a parabola:

$$\Sigma_{11} = A(K-B)^2 + C = AK^2 - 2ABK + (C + AB^2)$$

5. Evaluate the emittance: $\epsilon_x = \sqrt{AC}/S_{12}^2$

Measure projected emittance only

Bunch length Measurement : RF Deflector

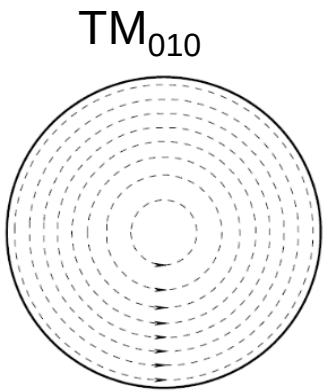

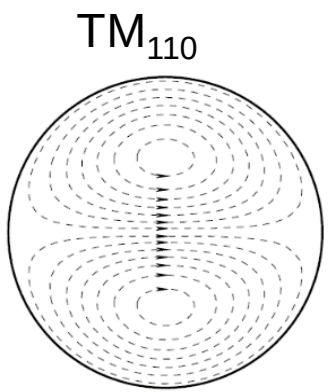

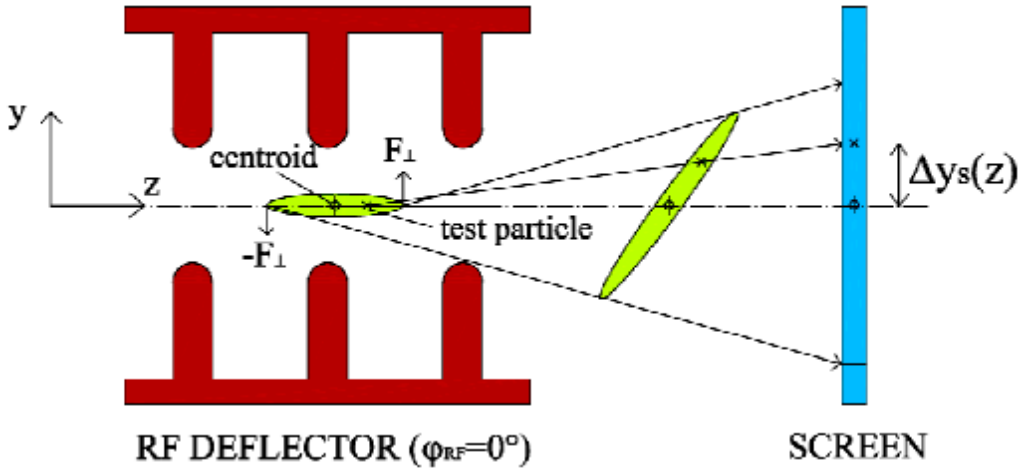

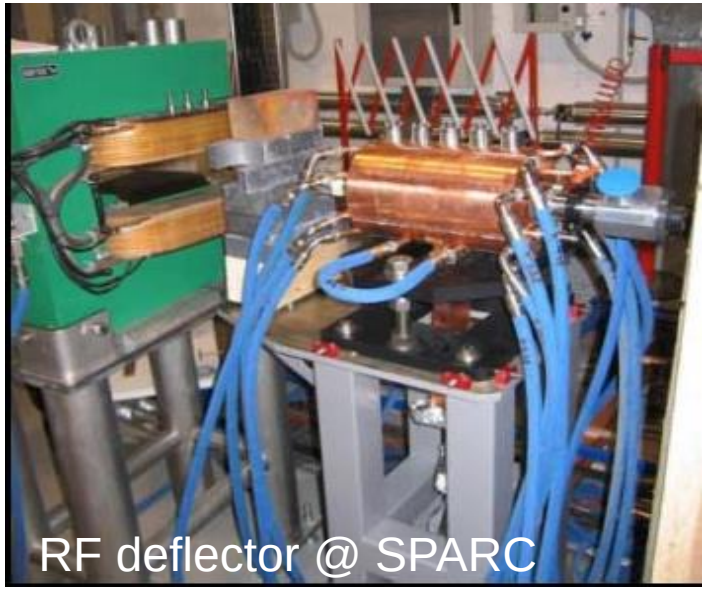

- Measure bunch length by using a TM_{11} like mode cavity to deflect the beam
- Single Shot Longitudinal Phase Space
- Resolution limited by beam size

國家同步輻射研究中心
National Synchrotron Radiation Research Center

Thanks for your attention!